

Review

^{19}F NMR in organometallic chemistry Applications of fluorinated aryls

Pablo Espinet*, Ana C. Albéniz, Juan A. Casares, Jesús M. Martínez-Ilarduya

IU CINQUIMA/Química Inorgánica, Facultad de Ciencias, University of Valladolid, 47011 Valladolid, Spain

Received 11 October 2007; accepted 20 December 2007

Available online 3 January 2008

Contents

1. Introduction	2180
2. Structural characterization using fluoroaryl groups	2181
2.1. General remarks	2181
2.2. Use of ^{19}F NMR to characterize atropisomers	2182
2.3. Use of ^{19}F NMR to study through-space coupling	2183
2.4. Use of ^{19}F NMR to study diastereomeric mixtures	2185
2.5. Use of ^{19}F NMR to detect unusual coordination modes	2186
3. Fluoroaryls in the study of dynamic processes	2188
3.1. General remarks	2188
3.2. Fluoroaryl rotation about C–M bonds	2189
3.3. Conformational changes in chelated ligands forming non-planar metallacycles	2193
3.4. Intramolecular ligand exchange and metallotropic processes	2193
3.5. Fluoroaryls as reporter ligands for remote fluxional processes	2195
3.6. Intermolecular exchange processes	2196
4. Fluoroaryl groups as tools in the study of fundamental organometallic reactions and mechanisms	2197
4.1. General remarks	2197
4.2. Studying simple reactions or catalytic steps with fluoroaryls	2198
4.3. Following reaction pathways by ^{19}F NMR	2199
4.4. Use of fluoroaryls to label several reaction partners	2201
4.5. ^{19}F NMR in C–F activation processes	2203
5. Conclusions	2205
Acknowledgements	2205
Appendix A. Abbreviations	2206
References	2206

Abstract

The applications of ^{19}F NMR in the study of a number of problems in organometallic chemistry are illustrated with relevant cases, paying special attention to the case of molecules containing fluorinated aryls. These are used as reporter groups of molecular symmetry, fluxional processes, and chemical changes, and help in the study of many fundamental organometallic processes.

© 2007 Elsevier B.V. All rights reserved.

Keywords: Nuclear magnetic resonance; Fluoroaryl; Fluorinated group; Chemical exchange; Fluxionality; Kinetics; C–F cleavage

1. Introduction

The ^{19}F nucleus shares many properties with ^1H : (i) the same nuclear spin $I=1/2$; (ii) almost the same high natural abun-

* Corresponding author. Tel.: +34 983423231; fax: +34 983423013.
E-mail address: espinet@qi.uva.es (P. Espinet).

dance ($^1\text{H}=99.98\%$; $^{19}\text{F}=100\%$) and similar gyromagnetic ratio ($\gamma(^{19}\text{F})/\gamma(^1\text{H})=1.062$), leading to not very different receptivity ($^1\text{H}=1$; $^{19}\text{F}=0.835$); and (iii) short spin-lattice relaxation times (a few seconds or less). Despite these similarities, there are some important differences in the NMR parameters of the two nuclei: [1] (i) the range of usual chemical shifts is much higher for ^{19}F (about 500 ppm) than for ^1H (about 10 ppm); (ii) the spin–spin interactions of ^{19}F nuclei are also larger than the corresponding interactions between protons; (iii) often the ^{19}F – ^{19}F coupling is transmitted not only through bonding electrons, but also by a direct *through space* mechanism; (iv) solvent effects influence ^{19}F resonances far more strongly than ^1H resonances and solvent induced shifts of 5 ppm and higher are not unusual.

It is clear from these features that ^{19}F NMR spectroscopy offers a number of advantages (not counterbalanced by any important disadvantage) as compared to ^1H spectroscopy: (i) the large range of chemical shifts usually produces well separated signals and first order spectra; (ii) for the same reason, fluxional or chemical exchange processes appear as slower processes when monitored by ^{19}F than by ^1H ; (iii) ^{19}F NMR spectra can be recorded in non-deuterated solvents and offer a clean window without solvent interference; (iv) additionally, the presence of fluorinated substituents often increases the solubility of the compounds to be studied. In fact, the utility of the fluorine labeling approach for NMR studies in Organometallic Chemistry and Biochemistry has been recognized for more than 40 years. The old 60 MHz machines, which had to focus on the most sensitive nuclei, were already provided with ^{19}F probes (e.g. the Perkin-Elmer R10 spectrometer at 56.4 MHz for ^{19}F) [2]. For a short period after the advent of FT NMR spectroscopy only dedicated laboratories were provided with ^{19}F probes, but nowadays the access to multinuclei probes that include the corresponding ^{19}F frequency is fairly general and the study of ^{19}F –“labeled” molecules, as a strategy to obtain extra and simpler information from NMR experiments, is gaining popularity. As a consequence the use of ^{19}F NMR spectra extends from the study of fluorinated molecules interesting by themselves, to those where the presence of F at chosen sites has been planned for it to serve as a reporter atom. Frequently this design comes with the additional bonus of modifying and simplifying the ^1H spin system and spectrum of the original non-fluorinated molecule.

Several groups, including ours, have shown for years the advantages of fluoroaryl ligands (Ar_F) to isolate and study organometallic complexes of many transition metals. In their studies ^{19}F NMR has been a most powerful technique for the elucidation of structures and the uncovering of dynamic processes in solution, as well as for kinetic studies. The most relevant

fluoroaryl ligands used are gathered in Scheme 1, and cover a number of situations: (i) Pf and Rf have both a C_2 symmetry axis, are chemically very similar, and can be used, as groups, in a way very similar to the use of isotope atoms in isotopic labeling studies; (ii) Fmes, which is also symmetrical, is characterized by a high steric demand and a high degree of axial protection in square–planar complexes; (iii) finally, 2- C_6BrF_4 and 3- C_6BrF_4 are examples of less symmetrical ligands (they lack a C_2 symmetry axis) with *ortho* substituents of different bulkiness, able to report on other features of the molecules.

This chapter is not aimed at being a comprehensive account of the use of ^{19}F NMR in organometallic chemistry. Our purpose is to illustrate its application to a variety of different problems and systems, as listed in the contents table. For this reason, studies reporting reiteration of the strategy for similar applications or similar chemical systems will not necessarily be referenced.

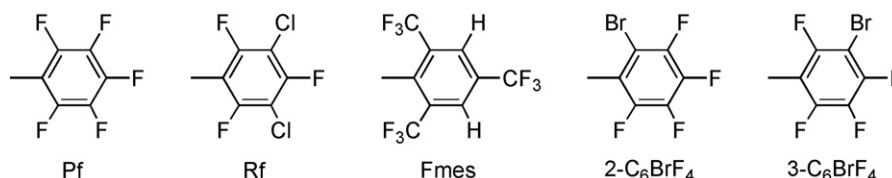
Although the most commonly used reference for ^{19}F NMR chemical shifts is CFCl_3 , other substances have been used in the literature. The chemical shift data in this study are given taking $\delta(\text{CFCl}_3)$ as 0 ppm, and positive δ -values downfield. Data from the literature have been converted to this convention when necessary.

2. Structural characterization using fluoroaryl groups

2.1. General remarks

The information in this section is mainly concerned with square–planar diamagnetic fluoroaryl complexes that, in the conditions of observation, are not undergoing any fast fluxional process that gives rise to chemical equivalence. Although the solid state X-ray structures of these fluoroaryl complexes often show the aryl rings making angles of about 70° with the coordination plane, the most stable conformation in solution is that with the aryl ring or rings roughly perpendicular to the coordination plane [3]. In the absence of fast fluxionality (this includes the exclusion of rotation around the M–Aryl ring) and in the case of aryl rings with a C_2 symmetry axis (e.g. Pf, Rf or Fmes) the fluorine substituents report on the equivalence or not of the two hemi-spaces above and below the coordination plane determined by the other ligands; in the case of aryl rings without a plane of symmetry (e.g. 2- C_6BrF_4 , or 3- C_6BrF_4) the aryl group produces inequivalence of these two hemi-spaces. Some examples will appear in the next pages.

Typical ranges of ^{19}F chemical shifts and ^{19}F – ^{19}F scalar coupling constants in Ar_F complexes are given in Table 1.



Scheme 1.

Table 1
 ^{19}F chemical shifts and F–F scalar coupling constants for the Ar_F ligands

Ar_F	Chemical shifts (ppm)		Scalar coupling constants (Hz)		
	Range	Order	<i>ortho</i> (3J)	<i>meta</i> (4J)	<i>para</i> (5J)
Pf	–100, –170	$\delta_2, \delta_6 > \delta_4 > \delta_3, \delta_5$	$J_{34} \approx 20$ $J_{56} \approx 20$	Very small	–
Rf	–75, –130	$\delta_2, \delta_6 > \delta_4$	–	Very small $J_{26} \leq 2.5$	–
Fmes ^a	–50, –65	$\delta_2, \delta_6 > \delta_4$	–	Very small	–
2- C_6BrF_4	–100, –170	$\delta_6 > \delta_3 > \delta_5 > \delta_4$	$J_{34} \approx 21$ $J_{45} \approx 20$ $J_{56} \approx 32$	Very small	$J_{36} \approx 11$
3- C_6BrF_4	–80, –170	$\delta_2 > \delta_6 > \delta_4 > \delta_5$	$J_{45} \approx 20$ $J_{56} \approx 31$	3–4	$J_{25} \approx 11$

^a δ_x and the coupling constants refer to the corresponding CF_3 groups.

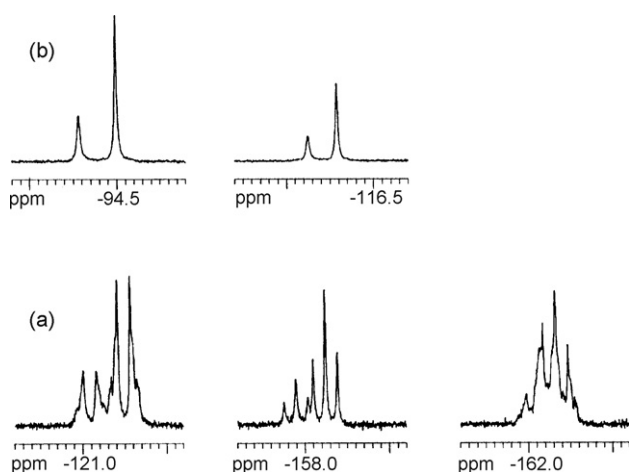


Fig. 1. ^{19}F NMR (CDCl_3 , 282.35 MHz) spectra of a mixture of *cis*- and *trans*- $[(\text{tht})\text{RPd}(\mu\text{-Cl})_2\text{PdR}(\text{tht})]$ ($\text{R} = \text{Pf}$ (a), Rf (b)) recorded using the same conditions (8 mM solutions, 8 pulses). The predominant species are the *trans* isomers. Reproduced with permission from ref. [4]. Copyright 1998, Elsevier.

The simplest ^{19}F spectral pattern is expected when there is only one Ar_F ligand. The groups providing the simpler spectra are Rf and Fmes, which show two singlets (2:1) when the two halves of the aryl ring are equivalent or three singlets (1:1:1) if they are non-equivalent (unless other coupling is involved). The greater simplicity of Rf spectra compared to Pf (Figs. 1 and 2) [4], greatly facilitates the characterization of

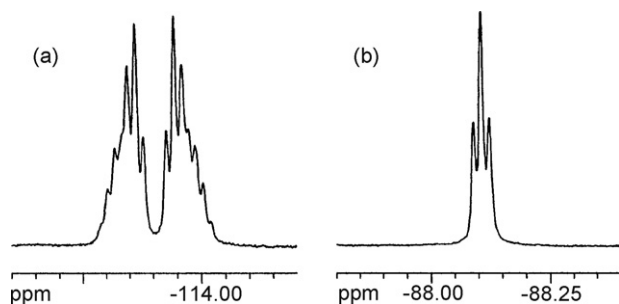


Fig. 2. ^{19}F NMR (CDCl_3 , 282.35 MHz) signals of the F_{ortho} atoms of *trans*- $[\text{PdR}_2(\text{PPh}_3)_2]$ ($\text{R} = \text{Pf}$ (a), Rf (b)). Reproduced with permission from ref. [4]. Copyright 1998, Elsevier.

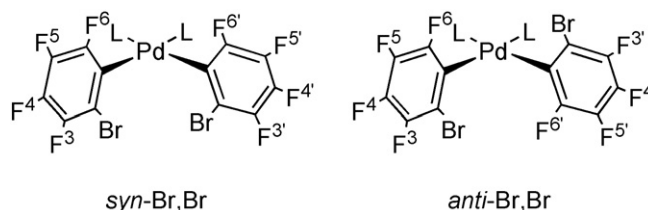
the complexes and the accomplishment of many studies, being particularly important when computer simulations (line-shape analysis) are involved. As shown in Fig. 1, the signals of Rf are singlets (instead of the multiplets observed for the Pf $\text{AA}'\text{MM}'\text{X}$ spin system), the signal-to-noise ratio is consistently better, and the resonances observed do not overlap. Even though ^{19}F is a nucleus with high receptivity, a better signal-to-noise ratio can save much time in kinetic experiments. In Fig. 2 the use of Rf instead of Pf also facilitates the observation of other coupling involved ($^4J_{\text{P-F}}$ in this case).

In spite of the advantages of Rf just mentioned, the number of studies that use Pf is, even now, much higher than with any of the other Ar_F ligands [5]. In fact, Pf sources were commercially available much earlier, PfBr is cheaper and more easily accessible than RfCl [6], and Pf derivatives are often more soluble. Yet, the reason for choosing Pf is often none of those but simple routine. Sometimes, however, there are good historical reasons: many modern studies lie on ^{19}F NMR identification of complex mixtures of compounds already reported and catalogued for Pf but not for Rf. This not being the case, the choice of Rf should have advantages.

2.2. Use of ^{19}F NMR to characterize atropisomers

In the course of our studies on restricted rotation about M-C(aryl) bonds, several palladium(II) complexes with the asymmetric aryl groups 2- C_6BrF_4 and 3- C_6BrF_4 were prepared, and a mixture of atropisomers (*syn*-Br,Br and *anti*-Br,Br) were found for most bisaryl complexes (Scheme 2) [7].

Assignment of all the ^{19}F signals was made using ^{19}F – ^{19}F COSY and homonuclear ^{19}F -decoupling experiments. The pres-



Scheme 2.

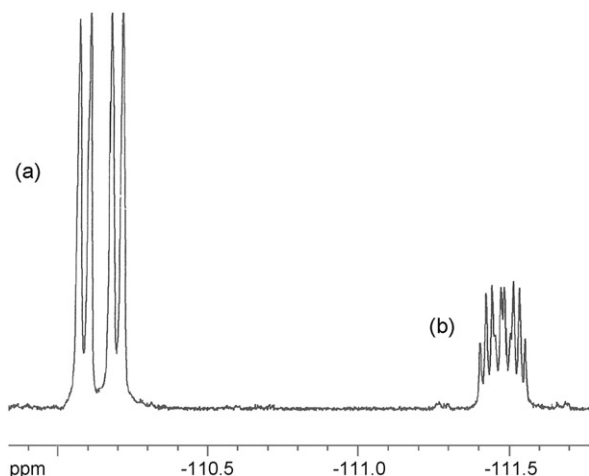


Fig. 3. ^{19}F NMR (CDCl_3 , 282.35 MHz) signals of the F^6 atoms of $\text{cis}[\text{Pd}(\text{2-C}_6\text{BrF}_4)_2(\text{COD})]$ (*anti*-Br,Br (a), *syn*-Br,Br (b)).

ence of strong inter-ring ^{19}F – ^{19}F coupling between *syn* F_{ortho} atoms (with a significant through space contribution) was clearly detected in the ^{19}F NMR spectra of the *cis* bisarylated complexes (Fig. 3), and their measurement proved useful to identify unambiguously the atropisomers formed.

Simple homodecoupling experiments allowed us to measure the inter-ring ^{19}F – ^{19}F coupling constants (Table 2), either directly when asymmetric ligands were involved, or analyzing the AA'XX' systems obtained in the case of symmetric ligands (see Fig. 4).

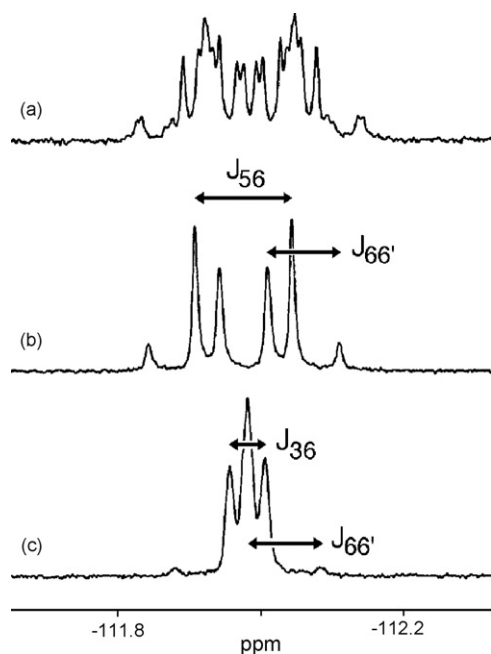


Fig. 4. ^{19}F NMR (CDCl_3 , 282.35 MHz, F^6 region) for $\text{cis-syn-Br,Br-[Pd}(\text{2-C}_6\text{BrF}_4)_2(\text{tht})_2]$: (a) initial signal; (b) signal under $\text{F}^3, \text{F}^{3'}$ irradiation ($\text{F}^5\text{F}^{5'}\text{F}^6\text{F}^{6'}$ spin system); (c) signal under $\text{F}^5, \text{F}^{5'}$ decoupling ($\text{F}^3\text{F}^{3'}\text{F}^6\text{F}^{6'}$ spin system). Analysis of spectra b and c allows the determination of the F^6 – $\text{F}^{6'}$ coupling constant. Reproduced with permission from ref. [7]. Copyright 1997, American Chemical Society.

A *syn:anti* ratio of atropisomers close to 1:1 is observed for the *cis*- and *trans*- $3\text{-C}_6\text{BrF}_4$ derivatives and for the *trans*- $2\text{-C}_6\text{BrF}_4$ complexes. In contrast the *anti* atropisomer is clearly preferred for the *cis*- $2\text{-C}_6\text{BrF}_4$ derivatives, particularly if the ancillary ligands span out of the coordination plane. The abundances observed correspond to the equilibrium distribution (atropisomerization is fast compared to the preparative times) and reflect the influence of the Br substituent on the stability of the complexes, which is important for the $2\text{-C}_6\text{BrF}_4$ derivatives, making the most hindered *syn*-Br,Br atropisomer noticeably less stable. The methodology of using asymmetric aryl groups to prove restricted rotation about the M–C bond has been adopted by other groups [8].

2.3. Use of ^{19}F NMR to study through-space coupling

The observation of through-space coupling is not uncommon in ^{19}F NMR spectroscopy [9], and it has been reported that the magnitude of the coupling depends on the distance between the interacting nuclei [10]. However, for many years this type of coupling, occurring on many reported *cis* bisfluoroaryl complexes, was not recognized [5]. The estimation of the scalar contribution to the inter-ring coupling between F_{ortho} atoms (0–3.5 Hz) indicates that most of the contribution found for *syn* F_{ortho} atoms (see Table 2) must be attributed to through-space coupling. The values of close F_{ortho} – F_{ortho} are in the range 52–9.9 Hz, which would correspond to $\text{F} \cdots \text{F}$ distances ranging from about 265 to about 320 pm. These distances are reasonable for the geometry of the complexes, and reveal the existence of distortions from an ideal square–planar coordination with the two aryl rings perpendicular to the coordination plane. The highest values of coupling are observed for the combination of *syn*-Br,Br atropisomers and non-planar ligands. This can be explained assuming that the crowding in the z -axis forces a tilt of the aryl groups in order to increase the distance between the Br atoms, bringing the *syn* F_{ortho} atoms closer to each other [7]. Following this recognition, ^{19}F – ^{19}F inter-ring coupling, largely through space in *cis* bis(fluoroaryl) complexes, facilitates their characterization and the carrying out of structural studies in solution, specially for the simple Rf and Fmes ligands.

Typical F_{ortho} patterns for static ^{19}F NMR spectra in *cis*- PdRf_2 square–planar complexes giving rise to AA'XX' spin systems are shown in Table 3 [11]. The spectra are very easy to recognize and correlate with the symmetry of the complex. Moreover, the pattern for Rf is maintained in cases of *cis*- PdPfRf systems and this information was used to characterize the heteroaryl complex *cis*- $[\text{PdPfRf}(\text{tht})_2]$ which is formed when mixtures of *cis*- $[\text{PdPf}_2(\text{tht})_2]$ and *cis*- $[\text{PdRf}_2(\text{tht})_2]$ are heated in CDCl_3 [12]. This complex has the same symmetry, hence the same spectral pattern for the $\text{F}_{\text{ortho}}(\text{Rf})$ signals shown in Table 3 entry (a).

More complex systems can be analyzed, as in the case of boat-shaped complexes containing pz, dmpz, mpz or indz double bridges. In the case of asymmetric azolates, head-to-head (HH) and head-to-tail (HT) arrangement of the two bridges can exist. The following complexes were made: $(\text{NBu}_4)_2[\text{Pd}_2(\mu\text{-NN})_2\text{Rf}_4]$ (NN = pz, dmpz), HH- and HT-

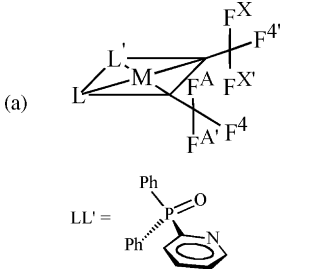
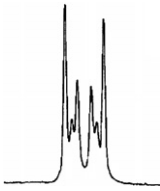
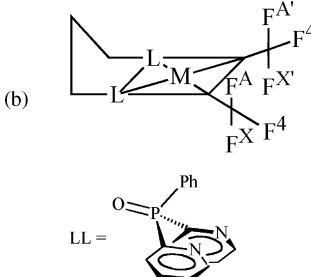
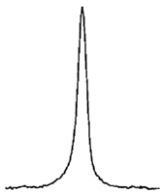
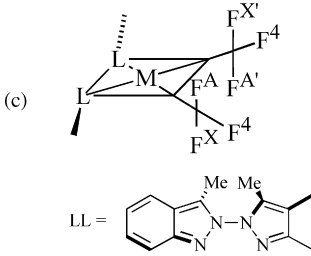
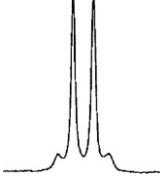
Table 2
 ^{19}F – ^{19}F inter-ring coupling in $\text{cis}[\text{Pd}(\text{C}_6\text{BrF}_4)_2\text{L}_2]$

L_2	Atropisomer	$\text{F} \cdots \text{F}$ close	J (Hz)	$\text{F} \cdots \text{F}$ distant	J (Hz)
$(\text{tht})_2^{\text{a}}$	<i>syn</i> -Br,Br	F^6 – $\text{F}^{6'}$	23.9	F^6 – $\text{F}^{6'}$	3.0
	<i>anti</i> -Br,Br				
COD ^a	<i>syn</i> -Br,Br	F^6 – $\text{F}^{6'}$	52.0	F^6 – $\text{F}^{6'}$	<3
	<i>anti</i> -Br,Br				
$(\text{CNMe})_2^{\text{a}}$	<i>syn</i> -Br,Br	F^6 – $\text{F}^{6'}$	22.5	F^6 – $\text{F}^{6'}$	3.7
	<i>anti</i> -Br,Br				
$\text{Me}_2\text{bipy}^{\text{a}}$	<i>syn</i> -Br,Br	F^6 – $\text{F}^{6'}$	25.6	F^6 – $\text{F}^{6'}$	4.0
	<i>anti</i> -Br,Br				
$\text{OPPhPy}_2^{\text{a}}$	<i>syn</i> -Br,Br- <i>anti</i> -Br,P	F^6 – $\text{F}^{6'}$	50.9	F^6 – $\text{F}^{6'}$	<2
	<i>anti</i> -Br,Br				
$\text{OPPhPy}_2^{\text{b}}$	<i>syn</i> -Br,Br- <i>syn</i> -Br,P	F^2 – $\text{F}^{2'}$	13.2	F^6 – $\text{F}^{6'}$	3.3
		F^6 – $\text{F}^{6'}$	26.2		
	<i>syn</i> -Br,Br- <i>anti</i> -Br,P	F^2 – $\text{F}^{2'}$	26.9		
		F^6 – $\text{F}^{6'}$	9.9		
	<i>anti</i> -Br,Br	F^2 – $\text{F}^{6'}$	25.5	F^2 – $\text{F}^{2'}$	3.3
		$\text{F}^{2'}$ – F^6	11.9	F^6 – $\text{F}^{6'}$	3.3

^a 2- C_6BrF_4 .

^b 3- C_6BrF_4 .

Table 3
 Static structure, appearance of the F_{ortho} signals and F_{ortho} – F_{ortho} inter-ring coupling of $\text{cis}[\text{PdRf}_2\text{L}_2]$ complexes with different symmetry^a

Complex	AA' part of $\text{AA}'\text{XX}'$ spin system (50 Hz)	J_{FF} (Hz) $J_{\text{AA}'}$, J_{AX} , $J_{\text{AX}'}$, $J_{\text{A}'\text{X}}$, $J_{\text{A}'\text{X}'}$, $J_{\text{XX}'}$
(a) 		0.0, 9.1, 3.2, 3.2, 9.1, 1.7
(b) 		^b , 0.7, 1.6, 1.6, 0.7, ^b
(c) 		0.6, –1.8, 8.2, 8.2, –1.8, 4.8

^a A schematic representation of Rf is used to show the geometrical arrangement and equivalences of Rf fluorine atoms.

^b $J_{\text{AA}'}$ and $J_{\text{XX}'}$ cannot be determined.

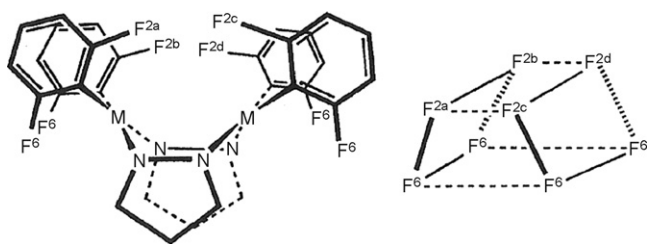


Fig. 5. Boat-shaped structure of a dinuclear azolato-bridged complex and a schematic representation of the spatial arrangement of the F_{ortho} atoms.

$(\text{NBu}_4)_2[\text{Pd}_2(\mu\text{-NN})_2\text{Rf}_4]$ (NN = mpz, indz), $(\text{NBu}_4)_2[\text{Pd}_2(\mu\text{-dpmz})(\mu\text{-NN})\text{Rf}_4]$ (NN = mpz, indz), and $(\text{NBu}_4)_2[\text{Rf}_2\text{Pd}(\mu\text{-NN})_2\text{PdPf}_2]$. Solution ^{19}F NMR data afford valuable structural information, which can be compared with structural data in the solid state. The ^{19}F – ^{19}F inter-ring coupling between the *endo* F_{ortho} atoms of different PdRf_2 fragments (F^{2a} , F^{2b} , F^{2c} , and F^{2d} in Fig. 5) are sensitive to the distortion produced by the presence of substituents in the bridging azolate ligands: these substituents reduce the dihedral angle between the coordination planes of the two metals, bringing closer these *endo* F_{ortho} atoms [13]. The coupling arising from this proximity require F_{ortho} signals to be treated as an eight nuclei spin system involving the four Rf groups.

The F_{ortho} region of the ^{19}F NMR spectrum of $(\text{NBu}_4)_2[\text{Pd}_2(\mu\text{-indz})_2\text{Rf}_4]$, where both isomers HT and HH are present, is shown in Fig. 6. The $J(^{19}\text{F}$ – $^{19}\text{F})$ values estimated by simulation of the static spectrum for the HT isomer are collected in Table 4. The simulation of the static spectrum for the HH isomer is more difficult and less informative and only the large values of $J(2a\text{--}2c) = J(2b\text{--}2d) = 75$ Hz are relevant. These values reveal the closer proximity of the *endo* F_{ortho} atoms in the less stable HH (giving a more crowded situation) than in the HT isomer.

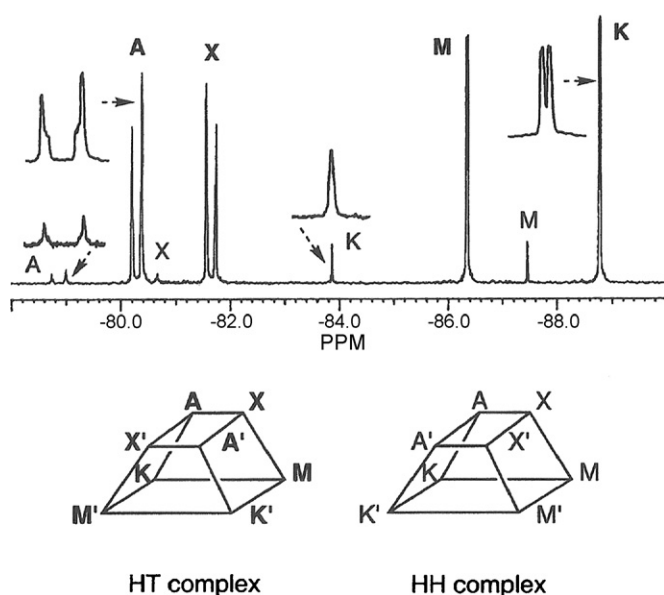


Fig. 6. F_{ortho} region of the ^{19}F NMR spectrum of $(\text{NBu}_4)_2[\text{Pd}_2(\mu\text{-indz})_2\text{Rf}_4]$ ($(\text{CD}_3)_2\text{CO}$, 282.35 MHz, 248 K) and assignment of the different signals. Reproduced with permission from ref. [13]. Copyright 2002, Elsevier.

Table 4

^{19}F – ^{19}F coupling (in Hz) in selected dinuclear azolato-bridged palladium complexes in $(\text{CD}_3)_2\text{CO}$ solutions

F–F	Complex/T (K)		
	A/248 ^a	B/195 ^b	C/195 ^b
2a–2b	5.4	0.0	0.0
2a–2c	48.0	105.0	112.6
2a–2d	0.0	0.0	0.0
2b–2c	2.5	16.3	13.0
2b–2d	48.0	59.5	62.6
2c–2d	5.4	5.0	5.8
6a–6b	8.8	9.7	10.6
6c–6d	8.8	35.5	37.6

Complex A: $\text{HT}(\text{NBu}_4)_2[\text{Pd}_2(\mu\text{-indz})_2\text{Rf}_4]$, Complex B: $(\text{NBu}_4)_2[\text{Pd}_2(\mu\text{-dpmz})(\mu\text{-mpz})\text{Rf}_4]$, Complex C: $(\text{NBu}_4)_2[\text{Pd}_2(\mu\text{-dpmz})(\mu\text{-indz})\text{Rf}_4]$.

^a Pyrazolate substituents are located near positions a and d.

^b Pyrazolate substituents are located near positions a, c and d.

With the previous data in hand and the information provided by ^{19}F – ^{19}F EXSY experiments, the static spectra of $(\text{NBu}_4)_2[\text{Pd}_2(\mu\text{-dpmz})(\mu\text{-NN})\text{Rf}_4]$ (NN = mpz, indz), which have the lowest symmetry with all the ^{19}F atoms chemically non-equivalent, can be easily interpreted and fully assigned (Fig. 7, Table 4).

A closely related study on several azolato-bridged complexes of group 10 metals with the Pf and 2,4,6- $\text{C}_6\text{F}_3\text{H}_2$ fluoroaryls has been published [14]. Both investigations of the correct meaning of the ^{19}F and ^1H NMR spectra lead to correct previous proposals of nonexistent fast monomer–dimer equilibria and Ar_F rotations.

The spectra of *cis*-bisarylated complexes containing chemically non-equivalent Fmes ligands reveal ^{19}F – ^{19}F through-space coupling between close *ortho*- CF_3 groups (8–10 Hz) and the lack of diagonal coupling between CF_3 groups of different Fmes ligands [15]. Trifluoromethyl groups belonging to Fmes ligands coordinated to different metal centers and placed at short distances can also show ^{19}F – ^{19}F through-space coupling as observed in the complex depicted in Fig. 8. In this complex one of the CF_3 appears as non-coupled indicating that it is far from the rest of trifluoromethyl groups as was confirmed by the solid state X-ray structure.

2.4. Use of ^{19}F NMR to study diastereomeric mixtures

Diastereomeric mixtures of complexes are often difficult to characterize in ^1H NMR, since the similarity of the spectral

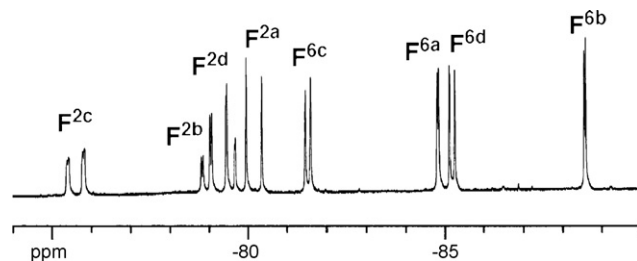


Fig. 7. F_{ortho} region of the ^{19}F NMR spectrum of $(\text{NBu}_4)_2[\text{Pd}_2(\mu\text{-dmpz})(\mu\text{-indz})\text{Rf}_4]$ ($(\text{CD}_3)_2\text{CO}$, 282.35 MHz, 195 K) and assignment of the different signals.

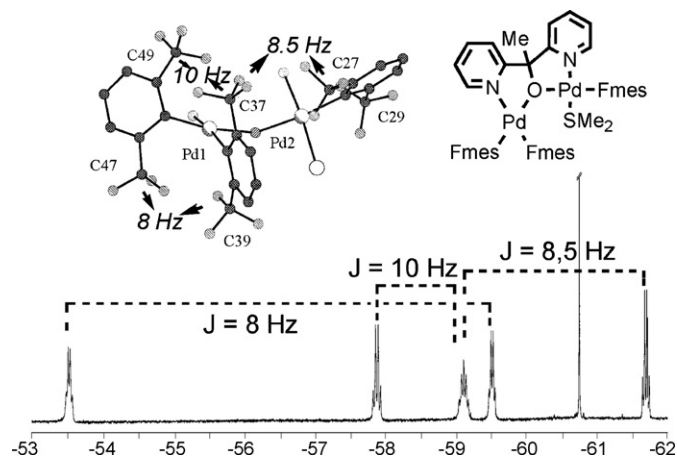


Fig. 8. ^{19}F NMR of $[\text{Pd}(\text{Fmes})_2(\mu\text{-}1\kappa\text{N}:1,2\kappa\text{O}:2\kappa\text{N-Py}_2\text{MeCO})\text{Pd}(\text{Fmes})(\text{SMe}_2)]$ (*ortho*- CF_3) in CDCl_3 at 298 K, showing through-space coupling. Reproduced with permission from ref. [15]. Copyright 2004, Elsevier.

pattern for the isomers leads to overlap or accidental coincidence of signals. The high sensitivity and wide range of ^{19}F chemical shifts often allows one to identify and study very similar isomers as, for instance, the four dimeric allyl palladium diastereoisomers in Fig. 9 [16]. These isomers have different stability and interconvert by bridge cleavage and rearrangement of the monomeric units. Both Pf groups are equivalent in each diastereoisomer, and the three distinct triplets observed at -50°C for the F_{para} resonance reveal the presence of three different isomers (out of the possible four species). Upon warming, interconversion of the species occurs and coalescence of the signals to just one F_{para} resonance is observed at 60°C .

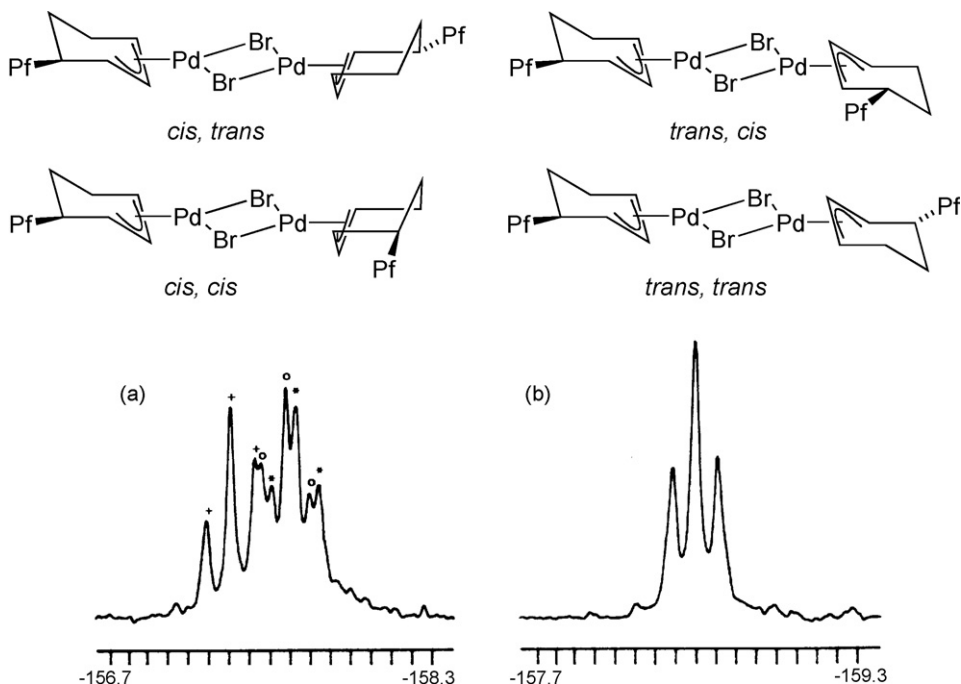


Fig. 9. The four possible diastereoisomers of a dimeric palladium complex with an asymmetric allyl moiety, and F_{para} signal of the complex at (a) -50°C (three triplets clearly visible) and (b) 60°C . Reproduced with permission from ref. [16]. Copyright 1990, American Chemical Society.

Heteronuclear ^1H – ^{19}F NOE effects have been used as a tool to characterize individual diastereoisomers. Hughes et al. have profusely used $^{19}\text{F}\{^1\text{H}\}$ HOESY experiments to assign the configuration of fluoroalkyl iridium derivatives [17–19]. An example is shown in Fig. 10 [20]. A C–F activation process in an iridium fluoroalkyl complex leads to a mixture of two diastereoisomers derived from a chiral Ir center and an asymmetric fluoroalkyl coordinated to the metal. The configuration and preferred conformation in the ground state for both diastereoisomers were determined by $^{19}\text{F}\{^1\text{H}\}$ HOESY experiments. Newman projections of one enantiomer of each diastereoisomer and relevant proton–fluorine NOE's are depicted in the Fig. 10. It turns out that one of them is the kinetic diastereoisomer and the other the thermodynamic one. The identification of the isomers led the authors to propose a mechanism for interconversion that involves epimerization in a cationic complex after the actual C–F bond cleavage.

2.5. Use of ^{19}F NMR to detect unusual coordination modes

Although very important as intermediates in many transmetalation processes, organometallic complexes with bridging aryl groups are rare among group 10 metals. The ease of aryl group transfer and reductive elimination in *bis* aryl derivatives often precludes the isolation of stable complexes of this type [21]. These reactions are slower for *ortho* substituted haloaryls and most of the scarce examples of dimeric palladium and platinum complexes with bridging aryls reported contain these groups [21–27]. ^{19}F NMR is useful to identify this structural feature, as the F_{ortho} resonances are strongly shifted downfield, compared to the terminal ones, as shown in Fig. 11 for $(\text{NBu}_4)_2[\text{Pt}_2(\mu\text{-Pf})_2\text{Pf}_4]$ [22]. Interestingly $^3J_{\text{F-Pt}}$ of the ^{195}Pt – Pt isotopomer is

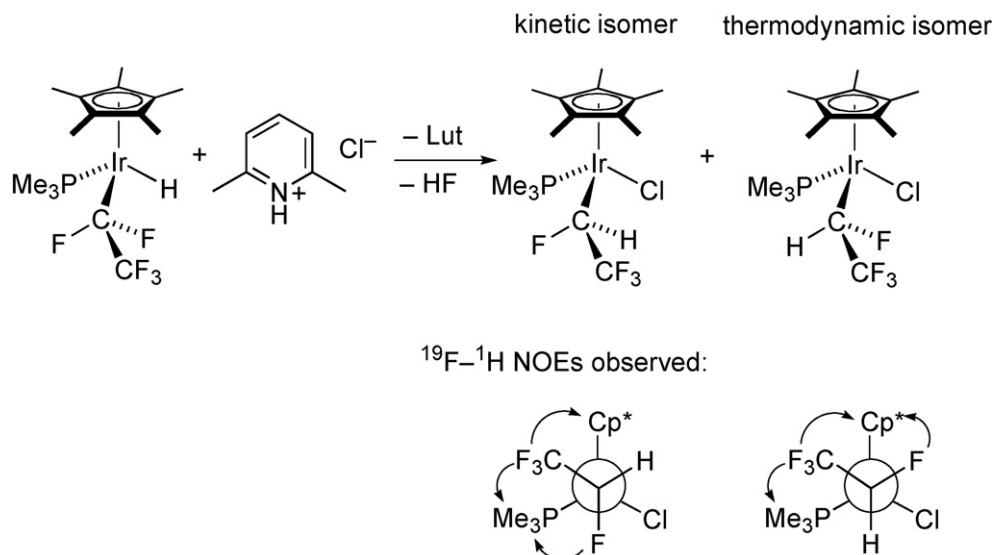


Fig. 10. Identification of a diastereoisomeric mixture by $^{19}\text{F}\{^1\text{H}\}$ HOESY experiments. Relevant NOE relations are shown.

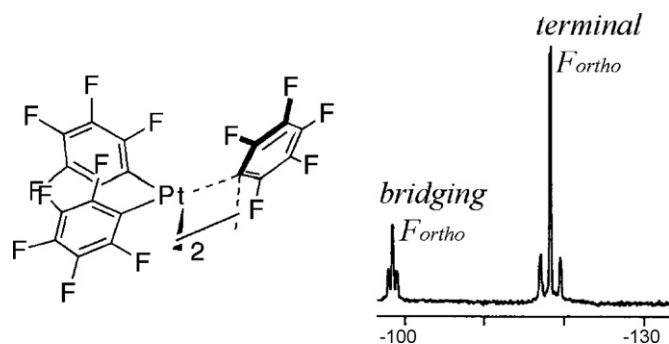


Fig. 11. ^{19}F NMR spectrum of $(\text{NBu}_4)_2[\text{Pt}_2(\mu\text{-Pf})_2\text{Pf}_4]$ in the F_{ortho} range. Reproduced with permission from ref. [22]. Copyright 1988, American Chemical Society.

clearly larger for the terminal fluoroaryls than for the bridging group.

The ^{19}F NMR spectrum of the rhodium complex depicted in Fig. 12 is also very informative, showing a pattern that reflects the loss of symmetry of the fluoroarene C_6F_6 , and two fluorine atoms coupled to ^{103}Rh and ^{31}P . This supports an η^2 -coordination mode of the arene [28,29].

Weak interactions of fluoroaryls with metals through $\text{M} \cdots \text{F}$ contacts have been detected in solution using ^{19}F NMR for the zwitterionic borate metallocenes in Fig. 13 [30]. In the ^{19}F spec-

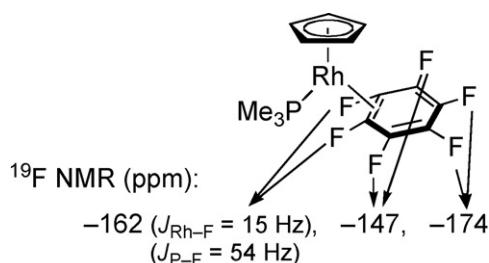


Fig. 12. ^{19}F NMR data for a Rh-bound $\eta^2\text{-C}_6\text{F}_6$.

tra of the Zr complex at -80°C a total of 14 separate signals for the 15 non-equivalent F atoms ($2F_{\text{meta}}$ are isochronous) are observed. All the signals appear in the chemical shift range -137 to -127 ppm (typical for F_{ortho} in pentafluorophenyl complexes), except one F_{ortho} resonance shifted to -209.9 ppm, assigned to a $\text{Zr} \cdots \text{F}$ interaction. Upon warming the complex becomes fluxional and coalescence occurs at about -30°C . An activation energy of $8.5 \text{ kcal mol}^{-1}$ for the $\text{Zr} \cdots \text{F}$ dissociation energy was estimated [31]. These contacts seem to play a protection role of the complex against deactivation when they are used as olefin polymerization catalysts. $\text{Zr} \cdots \text{F}$ interactions have also been detected by ^{19}F NMR between cationic zirconocenes and tetrafluoroarylborate anions [32].

Starting from an Ir complex containing a $\text{N-H} \cdots \text{F}$ hydrogen bond to a F ligand, the protonation of the amine substituent changes this interaction in such a way that in the resulting cationic complex the fluorine resonance appears at -178 ppm, strongly coupled to hydrogen ($^1J_{\text{F-H}} = 440 \text{ Hz}$, cf. $^1J_{\text{F-H}} = 52 \text{ Hz}$ in the starting complex). This suggests that the cationic complex should better be considered as a complex with the simplest fluorine-containing molecule, HF, as a ligand (Scheme 3, a) [33]. The observation of a $cis\text{-}^2J_{\text{F-P}}$ coupling of 12 Hz further indicated that the F atom is coordinated to Ir, ruling out the possibility of an uncoordinated HF moiety just H-bonded to the amino group. A different case is that of FHF^- complexes with the bonding

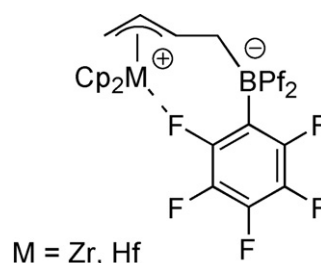
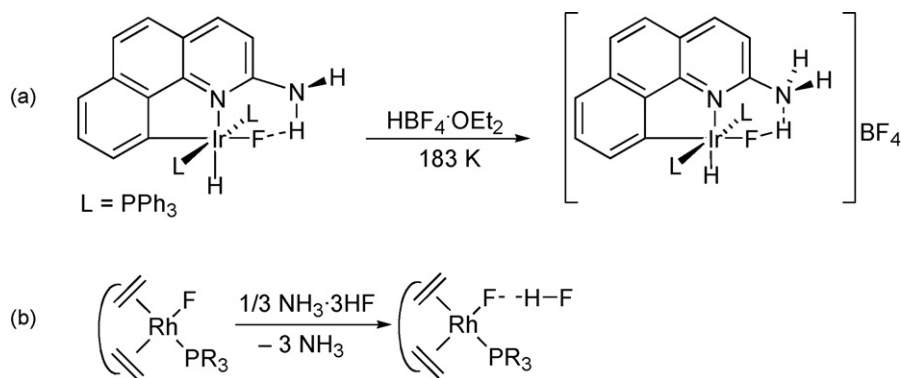


Fig. 13. $\text{M} \cdots \text{F}$ contacts in borate metallocene derivatives.



Scheme 3.

shown in Scheme 3 (b) for a Rh(I) complex (diolefin = COD). In this case $^1J_{\text{F-H}}$ for the F bound to Rh (32–41 Hz depending on the phosphine) is clearly smaller than $^1J_{\text{F-H}}$ for the terminal F (360–375 Hz) [34].

3. Fluoroaryls in the study of dynamic processes

3.1. General remarks

The difference in chemical shift between non-equivalent F signals in the same or in different aryl rings is usually fairly large (in Hz), certainly bigger than the usual differences between two non-equivalent signals in ^1H spectroscopy, which makes the fluxional processes “slower” in ^{19}F than in ^1H NMR spectroscopy. Thus, high exchange rates are required to produce the coalescence of the signals in dynamic systems. For instance, fluoroaryl systems in a medium field-strength spectrometer (300 and 400 MHz) show non-equivalent fluorine nuclei at related stereochemical positions (e.g. two *ortho* fluorine atoms), very often separated by 5–10 ppm, and higher differences are not unusual; in comparison *ortho* ^1H signals separated more than 2 ppm are rare. This means that it is possible to study dynamic systems, through ^{19}F NMR, that would exchange too fast in ^1H NMR.

When the course of the reactions can be monitored for minutes or longer times, the instant concentrations of reactants and products versus time are determined by accurate integration of their distinct signals in a sequence of spectra obtained at different reaction times.

In the slow exchange limit, the study is usually performed by saturation transfer or, more often, by magnetization transfer methods (MT). In complex systems undergoing multisite exchanges the 2D equivalent experiment (EXSY) is often preferred. For these experiments the lowest observable rate depends on T_1 [35]. Since $T_1(^{19}\text{F})$ values are not particularly long in fluoroaryls, typically 0.2–2 s (comparable to aromatic protons), MT transfer or EXSY experiments cannot be applied to the study of processes with very slow reaction rates.

The existence of through-space coupling makes it possible to study dynamic processes in which the internal motion does not change the chemical shifts but changes the spin system. This is the case of the rotation of inequivalent Rf groups each bearing chemically equivalent F_{ortho} , as in *cis*-[MRf₂(LL')] in which

LL' is a planar (or fast averaged planar) ligand (e.g. entry (a) in Table 3) [11]. In these complexes the only way to detect the rotation of the fluoroaryl group is the change in spin system from AA'XX' to A₂X₂ when going from the low rate to the high rate limits (Fig. 14). The through-space *J* coupling constants are typically about 15 Hz in *cis*-[MRf₂(LL')] complexes. Consequently the range of rotation rates observable by change in the spin system is quite narrow (the same order of magnitude as through-space *J*). Yet the method is of high value as it can detect exchange processes otherwise unobservable.

Different molecular dynamic processes may have the same spectroscopic effect; in that case the origin of the observed exchange cannot be unambiguously demonstrated. For instance, in square-planar complexes with Rf groups all the molecular processes that make groups at both sides of the coordination plane equivalent might be interpreted as a rotation of the Rf group around the C–M bond. This is the case of complexes [MXPf(dppf)] and [MXPf(dEpF)]. The observed coalescence of the F_{ortho} and the F_{meta} signals could be equally attributed to the

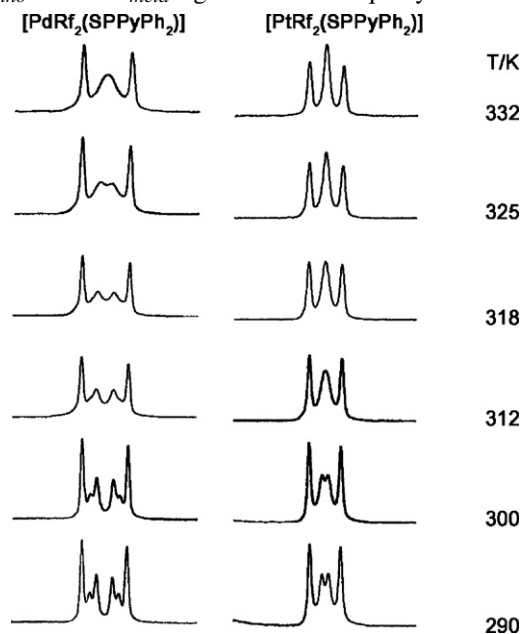
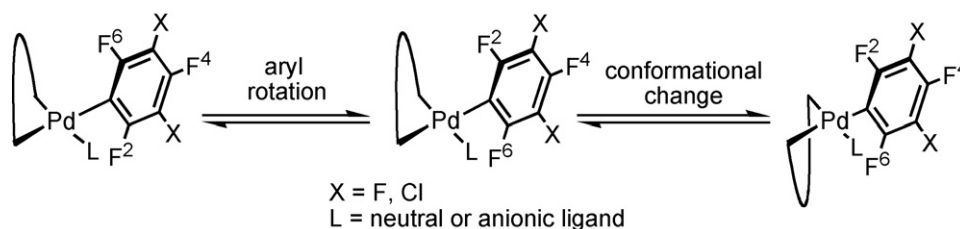


Fig. 14. Temperature dependence of the F_{ortho} AA'XX' part in the range 290–332 K for complexes [PdRf₂(SPPyPh₂)] in acetone-d₆ (left), and [PtRf₂(SPPyPh₂)] in CDCl₃ (right). Reproduced with permission from ref. [11] Copyright 1998, Wiley.



Scheme 4.

conformational change of the non-planar metallacycle formed by the chelate ligand, or to the Pf rotation about the Pd–C bond (Scheme 4) [36,14]. For this reason at a very early stage of the use of fluoroaryl systems for the study of dynamic processes, it became clear the necessity to establish when this rotation is plausible, and what are the kinetic values associated with this process.

A general classification of complexes $[M(Ar_F)_2(LL')]$ (LL' = chelate ligand) attending to their symmetry, their spin systems and the spectroscopic consequences of different dynamic processes has been reported [11].

3.2. Fluoroaryl rotation about C–M bonds

The observation of hindered rotation about M–aryl bonds in square–planar complexes of Pd and Pt, has been occasionally reported [37–44]. In complexes where this phenomenon is observed, the aryl group usually carries at least one *ortho* substituent (e.g. N=NPh, CH=NMe, Me, CH₂R, OMe), but restrictions leading to very slow rotation can also occur in aryl rings lacking *ortho* substituents but flanked by bulky ligands in the coordination plane, as in $[Pt(C_6H_3-3,5-Br_2)I(DIOP)]$ [41]. The existence of atropisomers arising from hindered rotation about the M–aryl bond has been often reported for complexes $[M(Ar)I(LL)]$ (Ar = aryl, LL = diphosphine or diamine) [40–43], and $[M(Ar)(NCN)]$ [44].

Since the most stable conformation in a square–planar complex is that with the aryl group normal to the coordination plane, the aryl ligand can be used as a reporter of whether the coordination plane is or is not a symmetry plane in the NMR time scale, provided that its rotation has a sufficiently high energy barrier. Conversely, ancillary ligands introducing a dissymmetry in the molecule such that the coordination plane is not a mirror plane, should permit the study of the M–aryl rotational barriers. Understanding aryl rotation processes is important for the interpretation of the reactivity and selectivity in catalysis. For instance, the aryl rotation in chiral palladium complexes has been shown to be crucial for the chirality transfer in the synthesis of dihydroquinolines [43].

The conditions for easy rotation of non-fluorinated aryls have not been well established, presumably because of the limited information obtained from ¹H NMR aromatic signals. A full kinetic study determining the activation parameters for the rotation (ΔG^\ddagger , ΔH^\ddagger , and ΔS^\ddagger) has been made only in the case of $[Pt(Ar)_2(COD)]$ (Ar = 2-(CH₂OMe)-5-R-C₆H₃; R = H, Me) [37], whereas only ΔG^\ddagger at coalescence temperature has been determined for $[Pt(Ar)Cl(COD)]$ [37a], $[Pd(C_6H_4-$

2-X)(η^5 -C₅H₄R)L] (X = N=NPh, CH=NMe) [38], and for $[Pd(C_6H_4-CH_2CH_2OH-p)Br(tmeda)]$ [40]. A much more complete picture has been reached with fluorinated aryls, such as Pf or Rf.

The hindrance to rotation in fluoroaryl octahedral complexes [45], was reported earlier than for square–planar complexes [46]. The latter was first observed in $[PtRCl(dcy)]$ (R = Pf, *p*-MeOC₆F₄) and $[Pt(p\text{-MeOC}_6\text{F}_4)_2(dcy)]$ (apparently rigid at room temperature). The hindrance was attributed to the rotation involving unacceptably close H⋯F approaches (<1 Å). The lack of rotation in $[PdPf_2(DMBI)]$ [47], $[PdPfBr(DMBI)]$ [47], and $[PdRf_2(DMBI)]$ [11], was argued to prove the lack of planarity in the coordinated 3,3'-dimethyl-2,2'-biindazole, in contrast with the planarity of their 5,5'- or 7,7'-isomers (Table 3, entry (c)). Non-equivalence of the two *F*_{ortho} at room temperature was also observed, for instance, in $[PdPf(PPh_3)_2(\mu\text{-OH})(\mu\text{-NHC}_6\text{H}_4\text{X-}p)]$ [48], $[PdPf(8\text{-methylquinoline})_2(\mu\text{-bipy})]$ [49], or $[Pd_3(\mu_3\text{-SPPH}_2)_2Pf_2L(PPh_3)_2]ClO_4$ (L = orthometallated ligand) [50].

There are many reports on Pf derivatives of Pd and Pt showing temperature-dependent ¹⁹F NMR spectra (equivalent to the effect of a rotation) assigned to the occurrence of fluxional processes not involving Pf rotation [36,51] but there are also many papers where free rotation of the Pf groups is argued [51b,51e,52,53], often as a defect assumption. A wrong assumption of free rotation may produce a misunderstanding of the symmetry of the complex, or can hide the true dynamic process responsible for the equivalence observed.

The case of the complexes $[PdPfX(SPPy_2Ph)]$ was chosen to assess when easy rotation about Pd–Pf bonds is plausible. The X-ray structure of one of its coordination isomers, $[PdPfX(SPPy_2Ph\text{-}N,S)]$ (with the SPPy₂Ph ligand coordinated through the sulfur and pyridyl nitrogen) was determined. The fluoroaryl ligand is arranged roughly perpendicular to the square coordination plane [54]. From the X-ray data it was easy to estimate the distances of the aryl *ortho* substituents to the donor atoms of the *cis* ligands in a hypothetical transition state for the rotation with the fluoroaryl ring in the coordination plane. In this transition state the *F*_{ortho} should get at a closer distance to the S and Br atoms than the sum of the corresponding Van der Waals radii. This indicates that the rotation is severely hindered and will require bond distortions. In effect, the aryl rotation, which could be measured by MT in CDCl₃ for the halocomplexes $[PdPfX(SPPy_2Ph\text{-}N,S)]$ (X = Cl, Br, I) (Fig. 15), is very slow in CDCl₃.

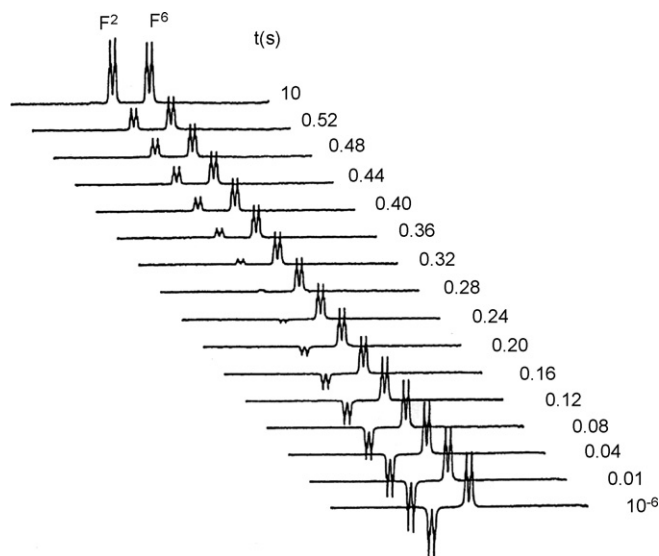


Fig. 15. Magnetization transfer experiment on $[\text{PdPfBr}(\text{SPPy}_2\text{Ph-N,S})]$ in CDCl_3 (F_{ortho}) revealing aryl rotation. Reproduced with permission from ref. [54]. Copyright 1995, American Chemical Society.

Table 5

Activation parameters for Pf rotation in $[\text{PdPfX}(\text{SPPy}_2\text{Ph-N,S})]$ in CDCl_3 (standard deviations in parentheses)

	X		
	Cl	Br	I
$\Delta G^\ddagger_{298}/\text{kJ mol}^{-1}$	71 (2)	68 (5)	65.4 (1.2)
$\Delta H^\ddagger/\text{kJ mol}^{-1}$	60.0 (1.2)	57 (3)	50.2 (0.6)
$\Delta S^\ddagger/\text{J K}^{-1} \text{mol}^{-1}$	−36 (4)	−38 (8)	−51 (2)

The activation parameters obtained show that ΔH^\ddagger associated with the rotation decreases as the size of the halide coordinated *cis* to the fluoroaryl ring increases (Table 5).

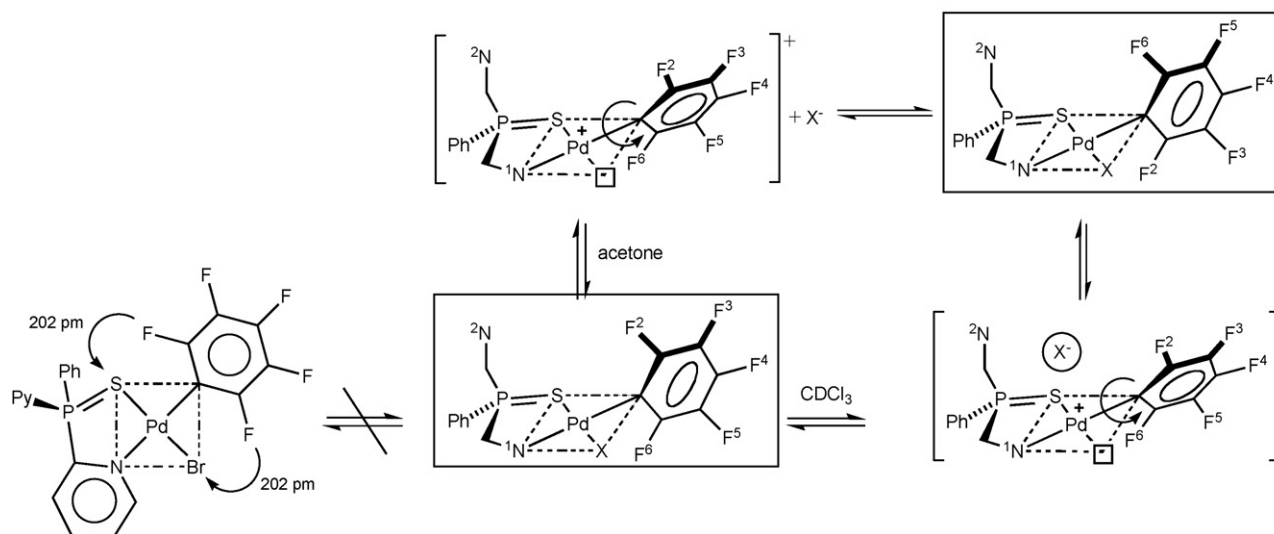
This trend is consistent with the proposed dissociation of the halide in a solvent in which the solvation enthalpy is small and

ΔH^\ddagger depends mainly on the Pd–X bond energy. Further support for halide dissociation came from the study of salt effects on the rotation rate (it is accelerated by the addition of salts to the medium), which suggest that, in the transition state, the cationic intermediate and the dissociated halide form a contact ion pair trapped in a cage of solvent (Scheme 5).

This example supports that rotation about the M–C_{ipso} bond of an aryl ring fluorinated in the two *ortho* positions often has a fairly high activation energy in square-planar Pd or Pt complexes. However, the same rotation is very fast in polar solvents, such as acetone (Scheme 5, upper pathway), suggesting that the dissociation energy is compensated by ion solvation.

Although mechanistically very informative, the above described strong dependence of the aryl rotation on the solvent or the ionic strength is not very usual. On the other hand, the dissociation of an anionic ligand is excluded in complexes *cis*- $[\text{Pd}(\text{Ar}_F)_2\text{L}_2]$. Hence, the study of the aryl rotation in systems of type $[\text{Pd}(\text{Ar}_F)\text{X}(\text{OPPy}_2\text{Ph})]$ (X = Ar_F, halide) was undertaken [7,11,55]. In these systems the fluoroaryl ring is always *cis* to a N atom, which has a much smaller Van der Waals radius than sulfur. With this ligand the *N,N*-chelation produces a boat conformation for the metallacycle that makes inequivalent both sides of the coordination plane (Scheme 6).

The fluoroaryl rotation in complexes $[\text{M}(\text{Ar}_F)_2(\text{OPPy}_2\text{Ph})]$ (M = Pd, Pt) is slow in CD_3Cl but can be properly studied by MT near and below room temperature, and by LSA at higher temperatures. The rotation process is not accelerated noticeably in acetone-*d*₆, CD_3CN , or $\text{DMSO-}d_6$, were different F_{ortho} signals were observed in each case. Table 6 gathers ΔG^\ddagger_{298} , ΔH^\ddagger , and ΔS^\ddagger values obtained for the rotation rates of these complexes in CDCl_3 . The rotation rate and ΔG^\ddagger_{298} are almost the same for analogous Pd and Pt complexes (Table 6, entries 1 versus 4, and 2 versus 5), varying with the halogen in the order $\text{Cl} > \text{Br} > \text{I}$ (Table 5), as expected for steric hindrance control. MT experiments on the H^6 signals of the Py groups show that they do not exchange at appreciable rate, and other possible mechanisms of F_{ortho} exchange, such as inversion of the chelating ligand and Pf



Scheme 5.

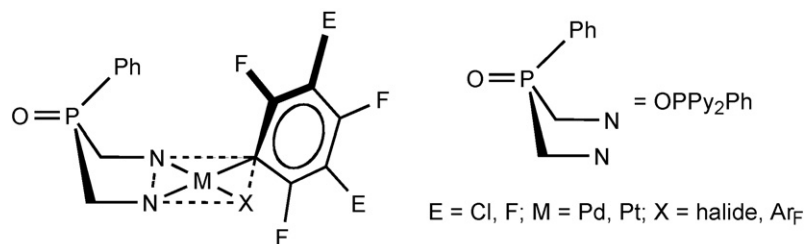


Table 6

Activation parameters for fluoroaryl rotation in complexes $[M(Ar_F)_2X(OPPy_nPh_{3-n})]$ and $[M(Ar_F)_2(L-L')]$ (standard deviations in parentheses)^a

Entry (ref.)	Compound	ΔG^\ddagger_{298} (kJ mol ⁻¹)	ΔH^\ddagger (kJ mol ⁻¹)	ΔS^\ddagger (J K ⁻¹ mol ⁻¹)
1 [55]	$[PdPf_2(OPPy_2Ph-N,N)]$	58.2 (0.4)	52.7 (0.4)	-18.2 (0.1)
2 [11]	$[PdRf_2(OPPy_2Ph-N,N)]$	60.8 (0.7)	57.6 (0.5)	-10.7 (1.6)
3 [55]	$[PtPfCl(OPPy_2Ph-N,N)]$	69.8 (0.9)	57.9 (0.8)	-39.8 (0.2)
4 [55]	$[PtPf_2(OPPy_2Ph-N,N)]$	57.3 (0.9)	51.8 (0.8)	-18.8 (0.3)
5 [11]	$[PtRf_2(OPPy_2Ph-N,N)]$	60.2 (0.2)	56.3 (0.1)	-13.4 (0.5)
6 [55]	$[PtPfCl(OPPy_3-N,N)]$	69.6 (0.5)	59.1 (0.3)	-35.0 (0.7)
7 [55]	$[PtPf_2(OPPy_3-N,N)]$	59.2 (0.6)	53.4 (0.5)	-19.5 (0.2)
8 [11]	$[PdRf_2(OPPyPh_2-O,N)]$	54.4 (0.5) ^b		
9 [11]	$[PdRf_2(SPPyPh_2-S,N)]$ ^c	75.1 (0.5) ^d		
10 [11]	$[PtRf_2(SPPyPh_2-S,N)]$	74.9 (0.5) ^d		
11 [11]	$[PdRf_2\{OPPyPh(NHTol-p)-O,N\}]$ ^c	55.1 (0.7)	45.4 (0.4)	-32.6 (1.8)
12 [11]	$[PtRf_2\{OPPyPh(NHTol-p)-O,N\}]$ ^c	52.4 (1.3)	42.9 (0.8)	-32 (3)
13 [11]	$[PdRf_2(DMBI)]$	85.92 (0.07) ^e		
14 [7]	$[Pd(3-C_6BrF_4)_2(OPPy_2Ph-N,N)]$		56.2 (1.2)	-12 (4)
15 [7]	$[Pd(2-C_6BrF_4)_2(OPPy_2Ph-N,N)]$	No rotation observed		

Solvent: CDCl₃.^a Unless otherwise stated.^b $\Delta G^\ddagger_{235.2}$.^c In acetone-d₆.^d $\Delta G^\ddagger_{324.7}$.^e $\Delta G^\ddagger_{329.1}$.

rotation in a three-coordinate intermediate, were also discarded. Moreover, for $[MPfX(OPPy_nPh_{3-n}-N,N)]$ complexes a plot of ΔG^\ddagger at 298 K (mean values when there are several compounds of the same type) versus the sum of covalent radii of the donor atoms of the two ligands flanking the rotating Pf group (i.e., $r_N + r_X$) gives a fairly linear correlation (Fig. 16). This allows

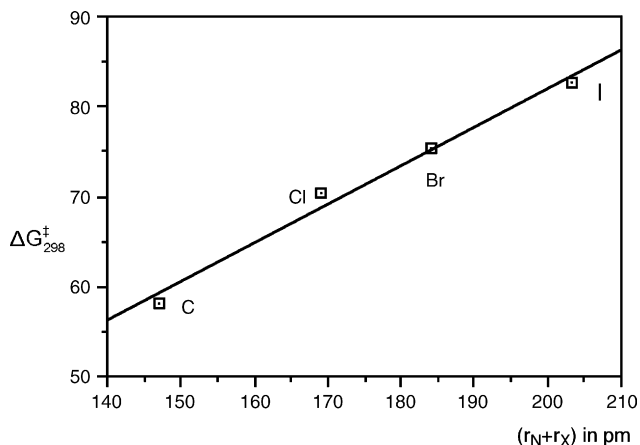


Fig. 16. Plot of ΔG^\ddagger at 298 K versus the sum of covalent radii of the donor atoms of the two ligands flanking the rotating Pf group. Reproduced with permission from ref. [55]. Copyright 1997, American Chemical Society.

to make some crude estimations of other barriers to rotation imposed by only the two coordinated atom flanking the Pf group and explain the reported behavior for other Pf complexes [55].

For chelate ligands making a quasi-planar metallacycle (Table 6 entries 8–12) in complexes $[M(Ar_F)_2(EPPyPhR')]$ (E = O, S, and R' = Ph; E = O, and R' = NHTol-*p*) the effect of the size of the atom coordinated *cis* to Rf is also evident, particularly when O and S are compared (entries 8 and 9). For these complexes (entries 9, 10 and 11, 12) the rotation rate is independent on the metal (Pd or Pt), showing that ligand bond breaking or associative ligand substitution are not involved in the rotation.

When the steric effect is different enough for both Rf groups, their rotation rates should also be different. The effect was clearly observed for $[PdRf_2\{OPPyPh(NHTol-p)\}]$ (Fig. 17). This example shows that the hindrance to rotation not necessarily comes from the donor atom only. In effect, N and O are similar in size, but the pyridyl ring lying close to the coordination plane invades the space needed for free rotation, producing a severe hindrance. The same reason applies to $[Pd(Ar_F)_2(DMBI)]$, which shows ΔG^\ddagger about 15 kJ mol⁻¹ higher than the complexes $[Pd(Ar_F)_2(OPPy_2Ph)]$ (entries 13 and 1, 2, 4, 5 in Table 6). In complexes $[Pd_2(Ar_F)_2\{\mu-P(C_2H_4Py)_nPh_{3-n}\}_2](BF_4)_2$ ($n = 2, 3$) the rotation of the fluoroaryl groups is slow as a result of the high steric hindrance on these dimers [56].

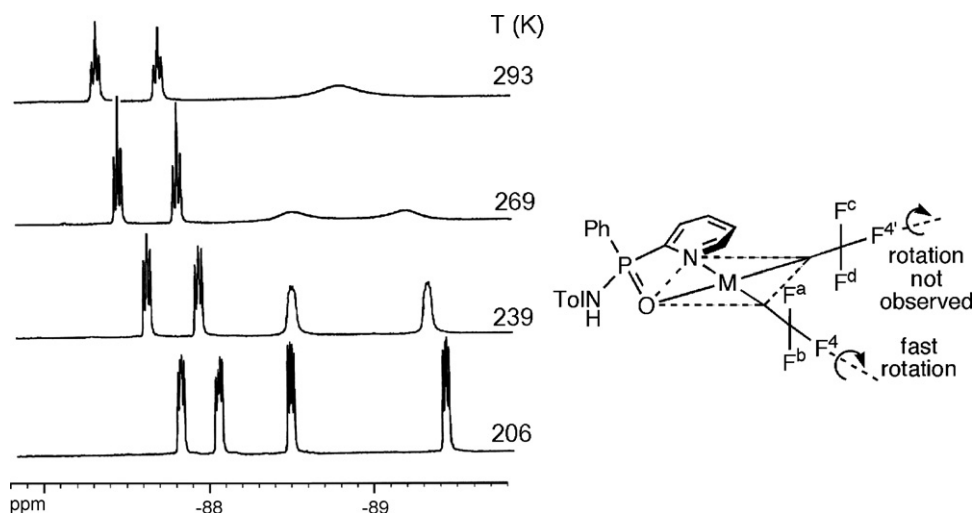


Fig. 17. Rotation of one Rf group while the other remains static in complex $[\text{PdRf}_2\{\text{OPPyPh}(\text{NHTol-}p)\}]$, as seen in the variable temperature ^{19}F NMR spectra in the F_{ortho} region. A schematic representation of Rf is used.

Aryl rotation in complexes with common ligands, such as isonitriles, phosphines, pyridines, etc., for which the coordination plane would be a symmetry plane with Rf or Pf groups, can be studied using asymmetrically substituted fluoroaryls such as *ortho* or *meta*-bromo-tetrafluorophenyl ($2\text{-C}_6\text{BrF}_4$, $3\text{-C}_6\text{BrF}_4$). With $3\text{-C}_6\text{BrF}_4$ the activation energy for rotation is comparable to that found with Pf in related complexes (Table 6, entry 14), although it involves exchange between the three possible atropisomers giving more complex spectra (Figs. 18 and 19). However, with $2\text{-C}_6\text{BrF}_4$ the rotation is very slow at the highest temperature available in CDCl_3 , showing that the size of the *ortho* substituent in the fluoroaryl ring is decisive for the rotation rate.

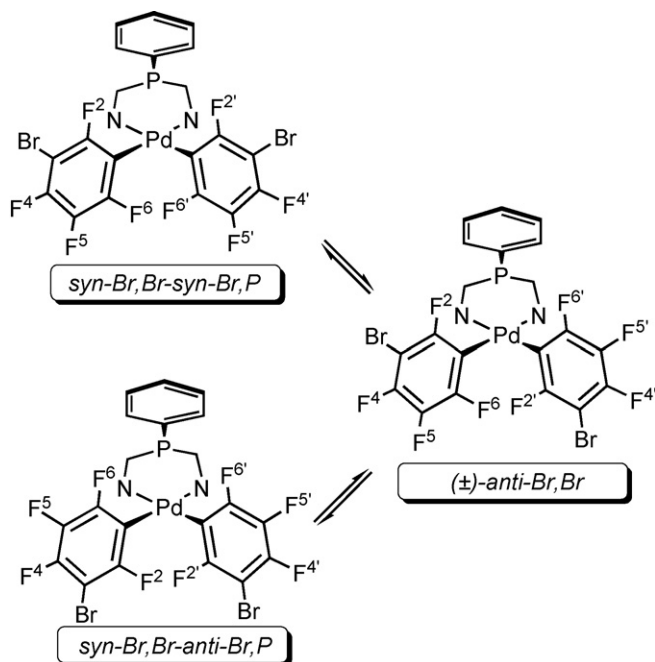


Fig. 18. Possible atropisomers related by rotation about Pd–ArF₃ bond for square-planar *cis* complexes with asymmetrically substituted aryls.

In complex *cis*- $[\text{Pd}(2\text{-C}_6\text{BrF}_4)(\text{tht})_2]$ the rotation rate of the fluoroaryl ring has been measured in CDCl_3 with different amounts of added tht [57]. The kinetic analysis of these data show that two rotation mechanisms coexist: (a) very slow rotation in the tetracoordinated square-planar complex, which

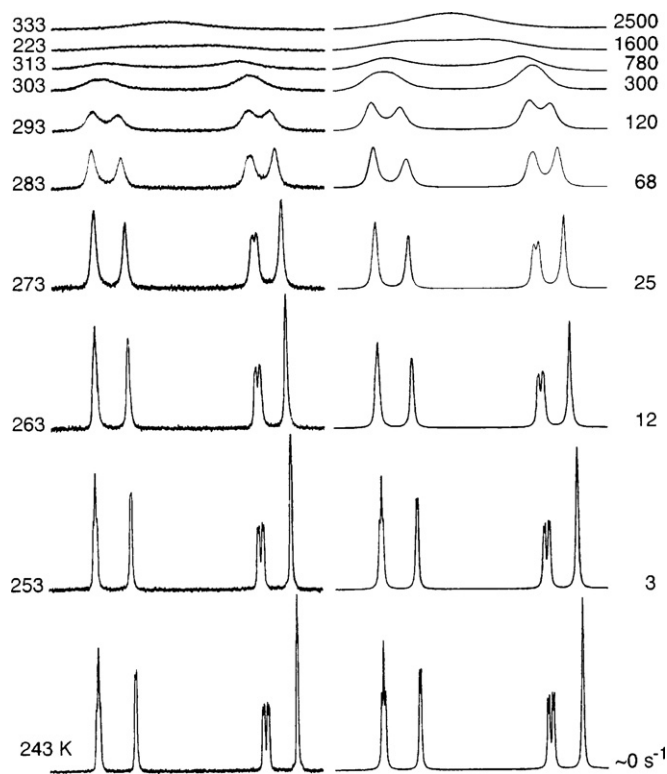


Fig. 19. Experimental (left) and simulated (right) ^{19}F NMR spectra (CDCl_3 , F^2 region) for $[\text{Pd}(\text{3-C}_6\text{BrF}_4)_2(\text{OPPy}_2\text{Ph-N,N})]$. First order atropisomerization constants are given at each temperature. The signals were assigned, starting from high field, to the atropisomers: *syn-Br, Br-syn-Br, P*, $(\pm)\text{-anti-Br, Br}$, *syn-Br, Br-anti-Br, P*, and $(\pm)\text{-anti-Br, Br}$. Reproduced with permission from ref. [7]. Copyright 1997, American Chemical Society.

becomes the only important mechanism when enough tht is added to the solvent; and (b) fast rotation in a three-coordinated complex formed by tht dissociation, which is the dominant pathway in solutions without added tht.

Some cases in the literature can be reviewed in the light of these results. For instance, it is very unlikely that Pf rings flanked in the complexes with donor atom of the size of chlorine or bigger are “freely rotating” and, if rotation is clearly observed, a dissociative mechanism should be taken into account. On the other hand, in many cases the rotation rate can be used as an “on plane hindrance gauge”, since it gives an idea of the bulkiness of the ligands *cis* to Ar_F in the coordination plane.

3.3. Conformational changes in chelated ligands forming non-planar metallacycles

The conformational changes of metallacycles formed by coordination of a chelating ligand can be easily studied by ¹⁹F NMR in fluoroaryl complexes. A fast conformational change creates an apparent symmetry plane (coincident with the coordination plane of the complex), producing the same effect than the aryl rotation on the ¹⁹F spectra. Consequently it can be studied only if it is faster than the aryl rotation.

Conformational changes are usually very fast in five membered metallacycles, but can be studied in six (or higher) membered metallacycles [58]. Complexes with bis(pyrazolyl)methane, tris(pyrazolyl)borates and related ligands, give boat-like metallacycle and tend to give one stable conformation with the bulkiest group towards the metal center. The same trend is found in complexes with 2-pyridylphosphine oxide or sulfide such [M(Ar_F)X(EPPy_nPh_{3-n}-N,N)] (M = Pd, Pt; X = Ar_F, halogen; E = O, S), for which only that conformation is found. However, in analogous chelating rings in which the phosphine is coordinated to a second metal center, such as [Rh(diene)(EPPy_nPh_{3-n}-N,N)] (E = PtPf₃) and [RhL₂(EPPy_nPh_{3-n}-N,N)] (E = AuPf; *n* = 2, 3; L₂ = (CO)₂, COD, tetrafluorobenzobarene), the two possible conformations are found [59,60]. In the platinum complexes, for the conformation that takes both metals close together, the rotation about the P–Pt

bond is very slow, rendering inequivalent the fluorine nuclei at both sides of the platinum coordination plane (Fig. 20). In the other possible conformation the platinum is freely rotating about this bond and fluorine equivalence is observed.

A boat-like metallacycle is also formed in complexes the (NBu₄)₂[Pd₂(μ-NN)₂Rf₄] (Section 2.2 and Fig. 5) [13]. The rate of the conformational change depends on the solvent used, and is slower in acetone-d₆ than in CDCl₃. This effect has been ascribed to the activation entropy change associated with solvent ordering when going from a polar ground state to a non-polar transition state. On the other hand, the fluoroaryl rotation is not solvent dependent. As consequence, the aryl rotation is the observable process in acetone-d₆ while the conformational change is observable in CDCl₃.

3.4. Intramolecular ligand exchange and metallotropic processes

The properties of Pf and Rf groups make them excellent reporter ligands for metallotropic shift between different donor atoms, a frequently observed phenomenon in multidentate nitrogen-donor ligands. Square-planar complexes of the type [MPf₂(terpy)] (M = Pd, Pt) exchange the metal-coordinated and uncoordinated nitrogen atoms in a process in which the 2-pyridyl exchange, measured in ¹H NMR, and the Pf exchange, measured by ¹⁹F NMR, have the same rate (activation parameters, obtained from LSA data, are gathered in Table 7, entries 1–3). A simultaneous change of the coordinated pyridine and the coordination site was proposed by a “tick-tock” twist mechanism (Scheme 7) [61]. Comparable values between ¹H and ¹⁹F data were found in analogous complexes with Me₂-TpzT (Table 7, entries 4 and 5) [62].

Similar complexes with substituted terpyridines such 4-methyl-4'-(4-chlorophenyl)-2,2':6',2''-terpyridine give rise to different isomers depending on which terminal pyridine is coordinated [63]. The ¹⁹F EXSY of the complex in Scheme 8 shows a double pairwise exchange between the four non-equivalent Pf groups (A ⇌ C, and B ⇌ D), which agrees with the “tick-tock” twist mechanism.

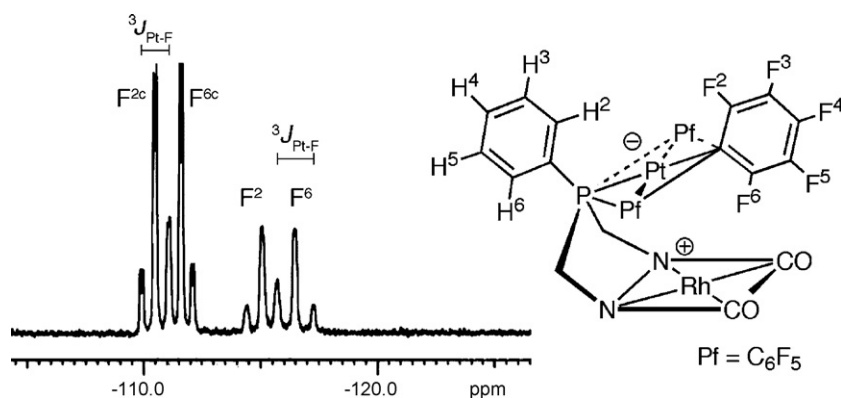
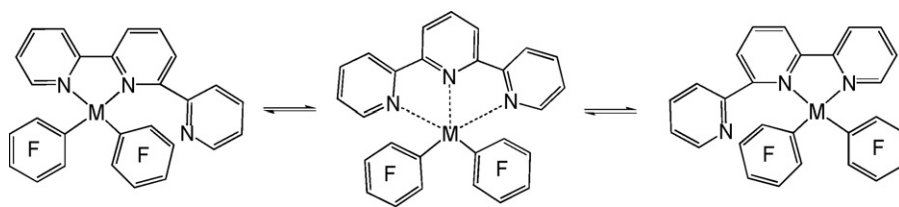


Fig. 20. Structure found in complex [PtPf₃(μ-PPy₂Ph)Rh(CO)₂] (for clarity only one Pf group is shown) and ¹⁹F NMR spectrum (only F² and F⁶ signals). The left signal corresponds to the two fluoroaryl rings *cis* to phosphorus (F^{2c} and F^{6c}). Reproduced with permission from ref. [55]. Copyright 2004, American Chemical Society.

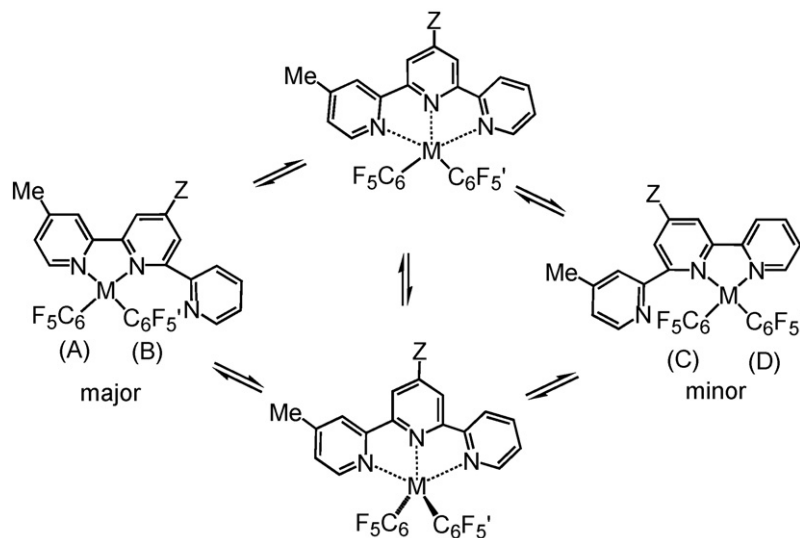
Table 7

Activation parameters for metallotropic exchange in complexes $[M(Ar_F)X(N,N,N)]$ (standard deviations in parentheses)^a

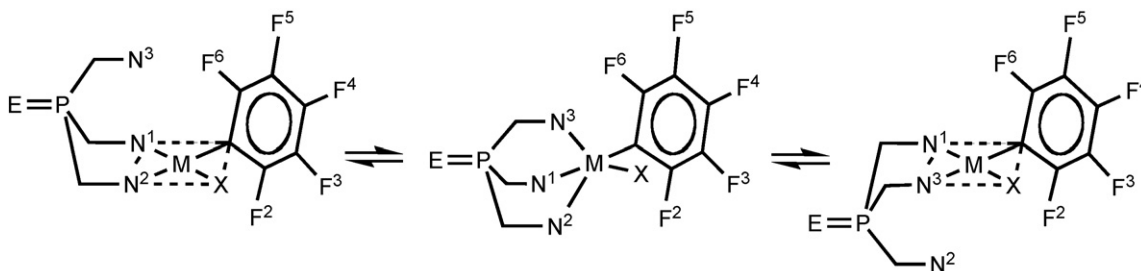
Entry (ref.)	Compound	ΔG^\ddagger_{298} ^a (kJ mol ⁻¹)	ΔH^\ddagger (kJ mol ⁻¹)	ΔS^\ddagger (J K ⁻¹ mol ⁻¹)
1 [61]	$[PdPf_2(terpy)]^{b,c}$	71.0 (0.2)	72.8 (1.2)	5.8 (3.3)
2 [61]	$[PdPf_2(terpy)]^{b,d}$	70.9 (0.3)	74.1 (2.0)	10.8 (5.5)
3 [61]	$[PtPf_2(terpy)]^{b,c}$	93.9 (0.7)	93.0 (2.9)	-3.2 (7.3)
4 [62]	$[PdPf_2(Me_2-Tpzt)]^{b,c}$	63.7	—	—
5 [62]	$[PdPf_2(Me_2-Tpzt)]^{b,d}$	64.2	—	—
6 [65]	$[Pd(C_6F_4CF_3)_2(TPT)]$	72.0 (0.2)	79.6 (1.1)	25.4 (3.2)
7 [65]	$[Pt(C_6F_4CF_3)_2(TPT)]$	102.7 (0.4)	—	—
8 [65]	$[Pd(C_6F_4CF_3)_2(TPP)]$	69.0	—	—
9 [65]	$[Pt(C_6F_4CF_3)_2(TPP)]$	117.7 ^e	—	—
10 [55]	$[PdPfCl(OPPy_3-N,N)]^c$	45.7 (1.0)	45.6 (0.9)	-0.3 (0.7)
11 [55]	$[PdPfCl(OPPy_3-N,N)]^d$	45.2 (1.6)	48.0 (1.2)	9.4 (1.5)
12 [54]	$[PdPfBr(SPPy_3-N,N)]^d$	44.2 ^f	—	—
13 [55]	$[PdPf_2(OPPy_3-N,N)]^c$	60.8 (0.2)	61.6 (0.2)	2.8 (0.1)
14 [55]	$[PdPf_2(OPPy_3-N,N)]^d$	58.2 (0.5)	57.0 (0.4)	-4.0 (0.2)
15 [55]	$[PtPfCl(OPPy_3-N,N)]$	76.6 (1.4)	76.5 (1.3)	-0.3 (0.3)
16 [55]	$[PtPf_2(OPPy_3-N,N)]$	Not observed	—	—
17 [56]	$[PdRfCl\{P(C_2H_4Py)_2Ph\}]^c$	59.5 (1.8)	47.9 (0.9)	-39.0 (3)
18 [56]	$[PdPfCl\{P(C_2H_4Py)_2Ph\}]^c$	60 (2)	47.7 (1.0)	-39.9 (3)

Solvent: $CDCl_3$.^a Unless otherwise stated.^b In $C_2D_2Cl_4$.^c From 1H NMR data.^d From ^{19}F NMR data.^e ΔG^\ddagger_{413} .^f ΔG^\ddagger_{243} .

Scheme 7.



Scheme 8.



Scheme 9.

The same exchange system has been reported for other multidentate planar N-donor ligands, such as TPT [64,65], TPP [64,65], 2,6-bis[(1-phenylimino)ethyl]pyridine [66], or Me₂-TpzT [62]. For ligands TPT, TPP and Me₂-TpzT, an additional metal-lototropic shift is found consisting of a metal exchange between the different nitrogen atoms of the central triazine or pyrimidine ring, in a movement that has been named “metal hurdling” [62,64,65], but this process has no effect on the ¹⁹F NMR spectra, and was studied by ¹H NMR.

Metallotropic shifts in non-planar multidentate ligands, such as polypyrazolylborates, are also common [67]. The exchange of coordinated and non-coordinated pyridines has been studied in complexes [MPfX(EPPy₃-N,N)] (M = Pd or Pt; X = Cl or Pf; E = O, S) [54,55], where the substitution follows a classical associative mechanism triggered by nucleophilic attack of the uncoordinated pyridine to the metal, perpendicular to the coordination plane. This mechanism is very sensitive to the *trans* effect of the other ligands and to steric effects. In [PdPfCl(OPPy₃-N,N)] and [PdPfBr(SPPy₃-N,N)] the pyridyl being substituted is that *trans* to the Pf group. Since the process produces the equivalence of the pyridyl groups involved in the exchange, but also the equivalence of F² and F⁶ (Scheme 9), the same activation energy values are found in ¹H and in ¹⁹F NMR (Table 7, entries 10 and 11). In complexes [MPf₂(EPPy₃-N,N)] the pyridine substitution is slower than in [MPfX(EPPy₃-N,N)] (X = halogen) (Table 7, entries 11, 12 and 13, and entries 15 and 16) due to the higher steric hindrance perpendicular to the coordination plane imposed by two fluoroaryl rings.

Complexes [PdPf₂(SPPy₂Ph)] and [PdRf₂(SPPy₂Ph)] provide a unique example of application of fluoroaryls to study the stereochemistry of the substitution processes [68]. In the two complexes the neutral ligand is N,S-bonded, [Pd(Ar_F)₂(SPPy₂Ph-S,N)], which makes the two fluorinated aryls in the molecule non-equivalent. The coordinated and non-coordinated pyridines exchange via a metallotropic shift analogous to those described above. The topological properties of any of these Ar_F groups report (through the F_{para} signals) that this substitution is accompanied by exchange of the two Ar_F groups in the complex, and that the incoming and leaving ligands approach and leave the palladium by the same face of the square-planar complex. The ¹⁹F EXSY spectrum in the F^{2,6} region shows a pairwise exchange, while the through space *J* coupling allows for stereochemical assignment of the fluorine signals (Fig. 21). The spectrum observed is the result of a dou-

ble substitution process in which the incoming pyridine occupies the sulfur site and the sulfur goes to the site of the leaving pyridine. In other words, this corresponds to a *turnstile* mechanism, which had not been observed before for Pd or Pt complexes. Isomerization reactions of the type [PdPfX(SPPy_nPh_{3-n}-S,N)] ⇌ [PdPfX(SPPy_nPh_{3-n}-N,N)] (X = halide or Pf, *n* = 2 or 3), also occurring in solution, are slower than pyridine exchange reactions and can be studied by ¹⁹F NMR at higher temperature than the other processes [54,68]. The turnstile process has been observed in the geometrically analogous complex [PdRf₂{OPPyPh(NHTol-*p*)-O,N}] using magnetization transfer experiments [11].

The exchange of coordinated ligands without the participation of pendant ends has been studied by ¹⁹F EXSY experiments in complexes (NBu₄)₂[Pd₂(μ-NN')₂Rf₄] and (NBu₄)₂[Pd₂(μ-NN')(μ-dmpz)Rf₄] (NN' = mpz, indz), in which HH and HT isomers exchange in CDCl₃ solution [13].

3.5. Fluoroaryls as reporter ligands for remote fluxional processes

The large range of ¹⁹F chemical shifts makes fluoroaryl ¹⁹F NMR sensitive to fluxions operating at remote sites that affect the symmetry of the complex. In [MPf₂(terpy)] (Scheme 7) and analogous complexes the rotation of the non-coordinated pyridyl leads to the equivalence of the F²–F⁶ and F³–F⁵ pairs (Fig. 22). At low temperature the rotation is arrested. The rotation rate was calculated by LSA of the ¹⁹F spectra [61,65]. Surprisingly, the activation energy for this process is significantly different for palladium (Δ*G*[‡] = 47.0 kJ mol^{−1}) and platinum (Δ*G*[‡] = 55.9 kJ mol^{−1}) complexes. In the stereochemically analogous system [PdPf₂(BIP)] the rotation of the non-coordinate imine arm about the C(imine)–C(pyridine) bond has been reported with a similar activation energy [66].

The detection through ¹⁹F NMR of the slow rotation of the uncoordinated 2-pyridyl ring about the C–P bond in bimetallic complexes [PdPf(4,4'-Me₂-bipy)(μ-PPy₃)Rh(diene)](BF₄)₂ (diene = COD or tetrafluorobenzobarrelene) has been reported [59]. In these complexes the pyridyl rotation, observed on the Pf signals, is additionally related to other processes at the rhodium center such as pyridyl exchange or olefin rotation.

Fluoroaryl groups in remote positions have been also used as reporter ligand, for instance in organometallic complexes with coordinated thioethers, in which coordinated sulfur inversion has been studied by ¹⁹F NMR [69].

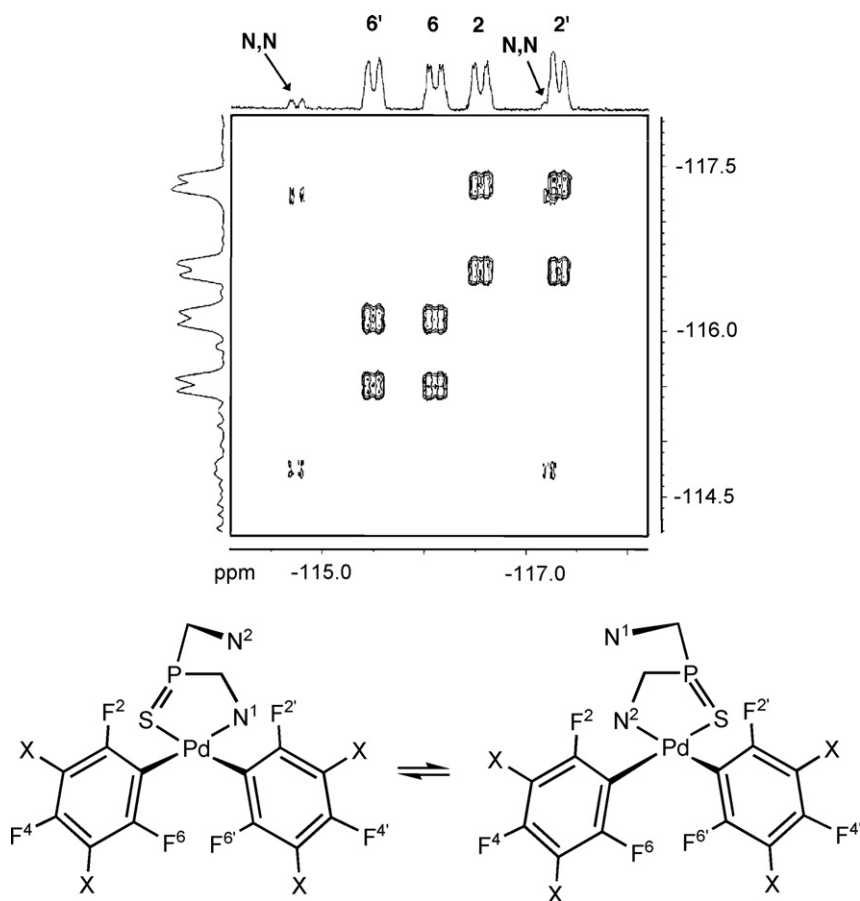


Fig. 21. ^{19}F EXSY experiment in complex $[\text{PdPf}_2(\text{SPPy}_2\text{Ph})]$ ($\text{F}^{2,6}$ region only). Numbering correspond to the N,S isomer, on which the exchange depicted below is observed. Minor peaks are observed for the N,N isomer, for which the cross-peaks observed are due to fluorine rotation.

3.6. Intermolecular exchange processes

The power of detection by ^{19}F NMR is shown in the following example. When complexes $\text{trans-}[\text{NiRf}_2\text{L}_2]$ ($\text{L} = \text{SbPh}_3$, AsPh_3 , AsCyPh_2 , AsMePh_2) are dissolved in wet acetone, iso-

merization (to give $\text{cis-}[\text{NiRf}_2\text{L}_2]$) and subsequent substitutions of L by $(\text{CD}_3)_2\text{CO}$ or by water occur, until the system equilibrates. Several complexes containing acetone and aqua ligands are formed [70]. The isomerization takes place in a few seconds at room temperature, and the substitution reactions are faster on

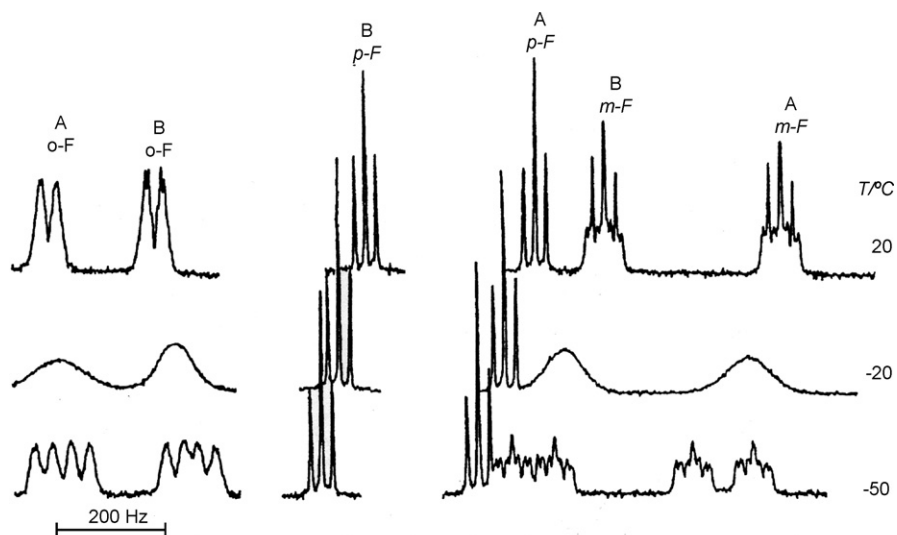


Fig. 22. ^{19}F NMR spectra of $[\text{PdPf}_2(\text{terpy})]$ in CD_2Cl_2 in the temperature range -50 to 20°C , showing the effects of restricted rotation of the pendant pyridyl ring on the *o*- and *m*-fluorine signals of both Pf rings. Reproduced with permission from ref. [61]. Copyright 1994, Royal Society of Chemistry.

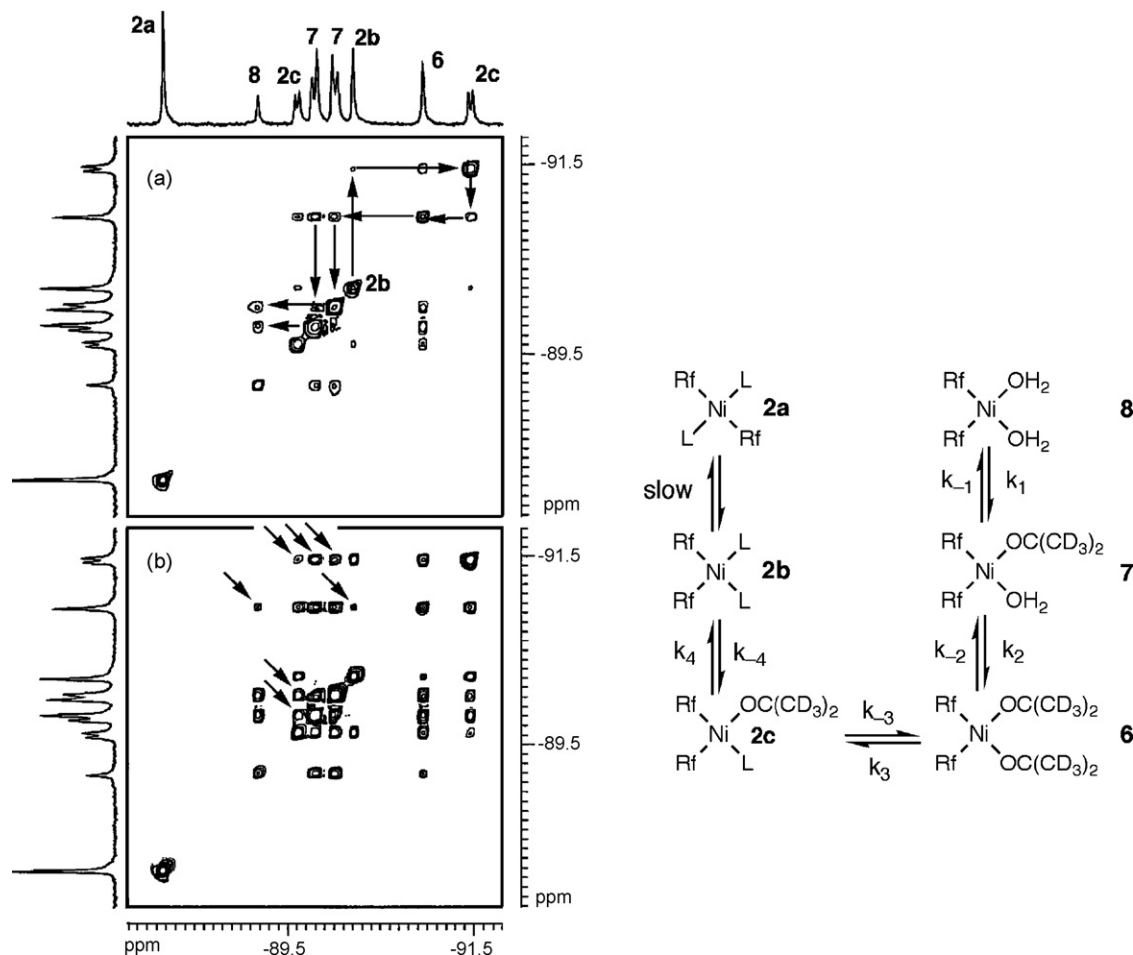


Fig. 23. ^{19}F EXSY experiments in the F_{ortho} region of a solution of *cis*-[NiRf₂(AsPh₃)₂] (**2a**) in wet acetone- d_6 at 217 K ((a) $t_m = 0.15$ s; (b) $t_m = 0.45$ s) and scheme of the exchange processes between the different species formed. Reproduced with permission from ref. [70]. Copyright 2007, American Chemical Society.

the *cis* isomer formed. The kinetics of the equilibria between all the species formed by partial or complete substitution of L ligands by water and by acetone- d_6 have been studied by ^{19}F EXSY experiments at 217 K (Fig. 23), and the exchange rates and rate constants have been calculated. Activation entropy values support an associative ligand substitution. The data obtained are the first available for square-planar nickel(II) aquacomplexes.

The intermolecular ligand exchange on complexes marked with Pf and Rf has been used to prove the dimer nature of the complexes [Pd₂Pf₂{ μ -P(C₂H₄Py)_{*n*}Ph_{3-*n*}}₂](BF₄)₂ and [Pd₂Rf₂{ μ -P(C₂H₄Py)_{*n*}Ph_{3-*n*}}₂](BF₄)₂, which are prepared independently and, when mixed in solution, afford the mixed complex [Pd₂PfRf{ μ -P(C₂H₄Py)_{*n*}Ph_{3-*n*}}₂](BF₄)₂, as shown by ^{19}F EXSY spectroscopy (Fig. 24) [56].

^{19}F EXSY and MT experiments have also been used to demonstrate that dimeric pyrazolate-bridged complexes are able to exchange palladium atoms with other complexes in solution [13]. The reaction [Pd₂(μ -NN)₂Rf₄] + [PdPf₂(thf)₂] \rightleftharpoons [Pf₂Pd(μ -NN)₂PdRf₂] + [PdRf₂(thf)₂] takes place in acetone- d_6 with an activation Gibbs energy $\Delta G^\ddagger_{298} = 77.62$ (0.08) kJ mol⁻¹.

4. Fluoroaryl groups as tools in the study of fundamental organometallic reactions and mechanisms

4.1. General remarks

Metal–fluoroaryl bonds are generally stronger than the analogous M–aryl bonds. The higher polarity of the M–C bond in these derivatives contributes to its higher strength. Fluoroaryls are also better π -acceptors when bonded to suitable electron-rich metal centers. The experimental result is that fluoroaryls allow to isolate stable organometallic complexes, including some intermediates in important catalytic processes. Moreover, fluoroaryl complexes are slower than aryl complexes in reactions involving the participation of the M–C bond. These features are ideal also for the study of reaction mechanisms other than the ligand exchanges already discussed in the previous chapter, which are the basis for the understanding of catalytic processes. In fact many organometallic reactions and elemental steps in catalytic cycles have been studied separately using these groups, contributing to a deeper and more complete understanding of the oxidative addition [71], the reductive elimination [72], the 1,2-alkene insertions [16,73–75], the 1,1-carbene insertions [76,77],

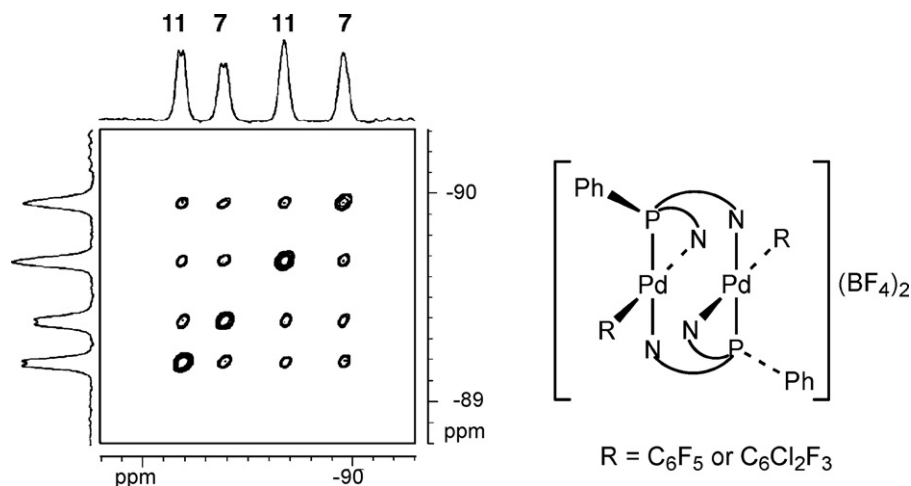


Fig. 24. ^{19}F EXSY spectrum of a mixture of $[\text{Pd}_2\text{Pf}_2\{\mu\text{-P}(\text{C}_2\text{H}_4\text{Py})_n\text{Ph}_{3-n}\}_2](\text{BF}_4)_2$ and $[\text{Pd}_2\text{Rf}_2\{\mu\text{-P}(\text{C}_2\text{H}_4\text{Py})_n\text{Ph}_{3-n}\}_2](\text{BF}_4)_2$ (**7**), showing signals from the mixed complex $[\text{Pd}_2\text{PfRf}\{\mu\text{-P}(\text{C}_2\text{H}_4\text{Py})_n\text{Ph}_{3-n}\}_2](\text{BF}_4)_2$ (**11**). Only the $\text{F}^{2,6}$ signals of the Rf group are shown (note that in both complexes Rf rotation is hindered). Reproduced with permission from ref. [56]. Copyright 1997, American Chemical Society.

the metal migration along hydrocarbyl chains [69,78–81], the transmetalations [82–85], the *cis*–*trans* isomerization [71,86], etc. Most of these studies deal with late transition metals, specially group 10.

^{19}F NMR has played a crucial role in these studies, as many reactions have been followed up in this way. When several species are being monitored, the wide ^{19}F chemical shift range reduces the problem of signal overlap, which is a great asset in the analysis of complex reaction mixtures, in conjunction with NMR spectra of other nuclei. On the other hand, F_{ortho} resonances are very sensitive to the nature of the atom bound to the *ipso* carbon of the fluoroaryl group. For instance, when $\text{C}\text{--}\text{Ar}_\text{F}$ bonds are formed from $\text{M}\text{--}\text{Ar}_\text{F}$ bonds, chemical shift changes higher than 20 ppm are found, revealing the fate of the Ar_F group (Fig. 25). As for the previous chapter, many reactions have been studied where Ar_F groups are not the reactive groups but report on other changes in the molecule. Using these convenient features, processes such as $\beta\text{--H}$ elimination and intramolecular alkene insertion in alkenyl chains [79], or transmetalation

and alkene insertion in alkenyl silanes [87], have been followed and the competition of different reactions has been detected and studied.

The importance of ^{19}F NMR is obvious in reactions where $\text{C}\text{--}\text{F}$ bonds are involved in reactivity. These processes lead to new fluoroaryls with different symmetry and number of fluorine atoms, a situation easily detected by this technique.

Examples of all these processes are discussed below.

4.2. Studying simple reactions or catalytic steps with fluoroaryls

One of the first examples that revealed the dramatic change in chemical shift of the F_{ortho} resonances when $\text{C}\text{--}\text{Ar}_\text{F}$ bonds are formed from $\text{M}\text{--}\text{Ar}_\text{F}$ systems is the insertion of isocyanides into $\text{Pd}\text{--}\text{Pf}$ bonds to give $\text{Pd}(\text{II})$ imido complexes (Scheme 10). The perfluorinated aryl allows the isolation of Pd complexes containing both groups (Pf and CNR) coordinated to Pd, which then undergo the insertion process upon heating [88–91]. The

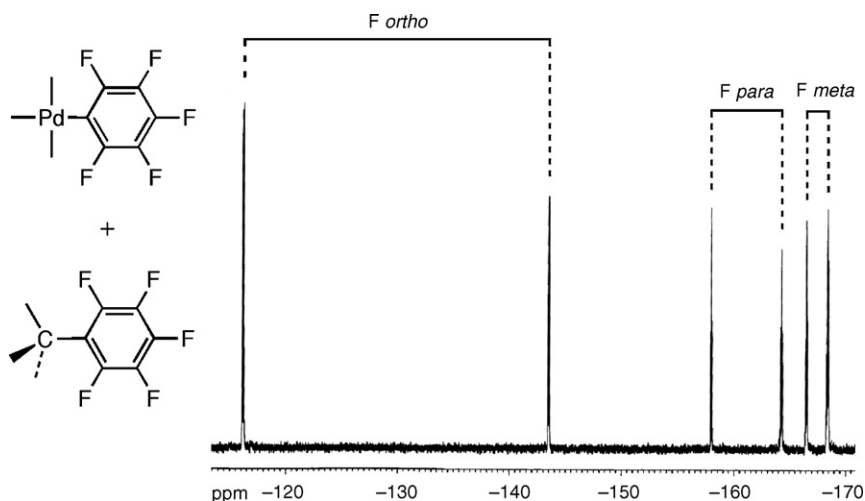
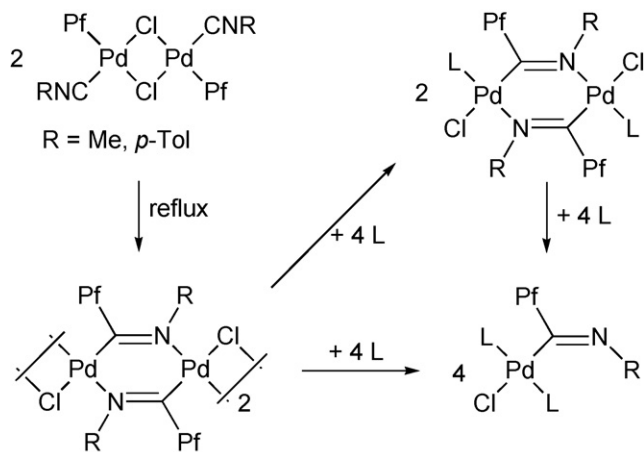


Fig. 25. Chemical shift differences for a Pf bound to carbon or to a metal.



Scheme 10.

initial product is a crown-shaped tetrameric complex. Controlled addition of L affords boat shaped dimers with the Pf and R substituents *cis* relative to the C=N bond in the bridging imidoyl ligands (see Fig. 26). Finally, more ligand splits these bridges to give terminal imidoyl groups, where the Pf and R substituents are *trans* relative to the C=N bond.

According to their structures the complexes with terminal imidoyls show free rotation of the Pf group, whereas the rest show restricted rotation, as illustrated for one dimer in Fig. 26.

Combining easy observation and higher stability of the complexes with fluorinated aryls, studies of reactions that are involved in catalytic cycles can be taken out of the cycle, and studied as isolated reactions. Thorough mechanistic studies made in this way on transmetalation processes in the Stille reaction have led to sound mechanistic proposals [82,83,85,92].

For instance, a most important step, common to most Pd -catalyzed reactions, is the oxidative addition of haloaryls (ArX) to PdL_n complexes to give a Pd(II) aryl complex. This reaction leads, with common aryls or under catalytic conditions, to *trans*- $[\text{PdXArL}_2]$ as the only observable product. Using $\text{Ar}_\text{F}\text{X}$

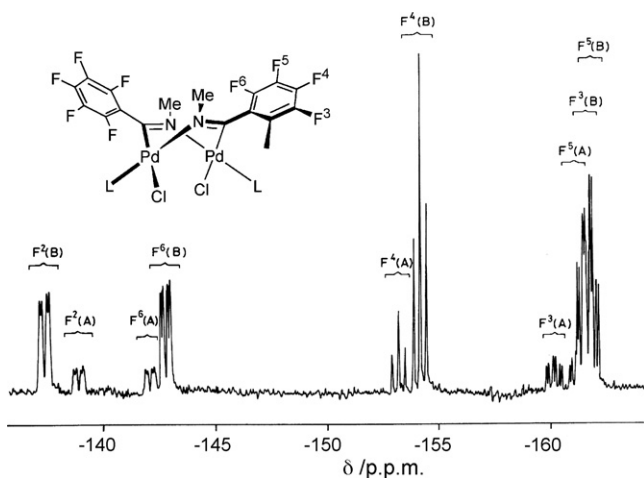
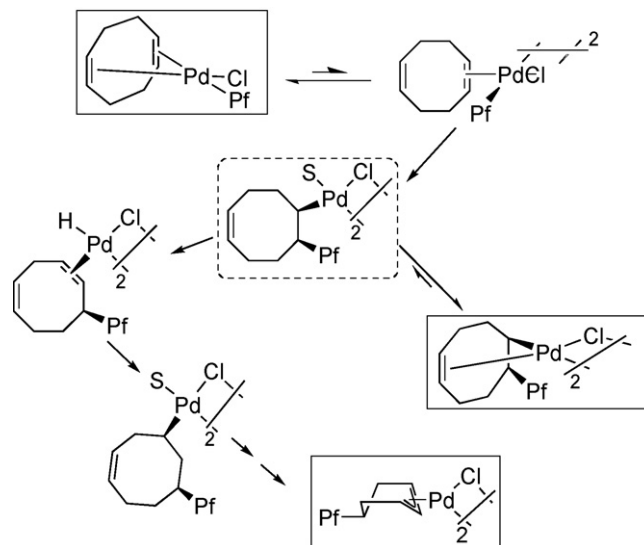


Fig. 26. Complete ^{19}F NMR spectrum of the complex shown ($\text{L} = 4$ -methylpyridine). Two types of Pf are observed ($\text{A}:\text{B} \approx 1:3$) due to isomers where L and Cl have exchanged their positions. Reproduced with permission from ref. [88]. Copyright 1982, Royal Society of Chemistry.



Scheme 11.

the oxidative addition was shown to proceed in two steps, giving quickly *cis*- $[\text{PdXArFL}_2]$, the actual product of oxidative addition, which then isomerizes more slowly to the *trans* derivative (Fig. 27) [71]. This supports a concerted, three center mechanism for the oxidative addition of aryl halides to Pd(0) . Rf was been used for its spectral simplicity, so that the conversion of *cis*- $[\text{PdIRf(PPh}_3)_2]$ (doublet of doublets for the F_{ortho} resonances) to the *trans* isomer (triplet) is easily followed. Kinetic studies lead to propose a complex four-pathway mechanism for the *cis-trans* isomerization.

4.3. Following reaction pathways by ^{19}F NMR

The insertion of COD in the Pd-Pf bond of $[\text{PdClPf(COD)}]$ (which can be isolated thanks to the slowness of the insertion reaction) can be monitored by ^{19}F NMR [73]. Two insertion products (framed in solid line in Scheme 11) are formed competitively from a common putative intermediate (framed in dashed line). This intermediate is stabilized by double bond coordination to give a σ, η^2 -enyl complex, or by Pd migration to form an allyl (thermodynamic product). This study proves (starting complex) or strongly supports (putative σ -alkenyl complex) this kind of intermediates in the Heck reaction and, more important, the stereoselective *cis* character of the insertion (1,2-addition of Pf-Pd to the olefin). Interestingly, in accordance with their structures, the σ, η^2 -enyl complex shows restricted rotation of the Pf group, whereas the η^3 -allyl complex displays free rotation.

Studies of closely related insertions of other alkenes or carbenes are aided by the straightforward identification of the fluorinated products [16,74,76]. The insertion of *R*-(+)-limonene into a Pd-Pf bond of $[\text{PdBrPf(NCMe)}_2]$ produces initially a σ, η^2 -enyl derivative as a mixture of two diastereoisomers (Fig. 28), which are distinctly detected in spite of their similar environment. They convert diastereoselectively into a mixture of two allyl palladium complexes (with overlapping signals) by Pd -migration along the chain. The process is impossible to study by ^1H NMR, and might be a bit confusing also by ^{19}F NMR,

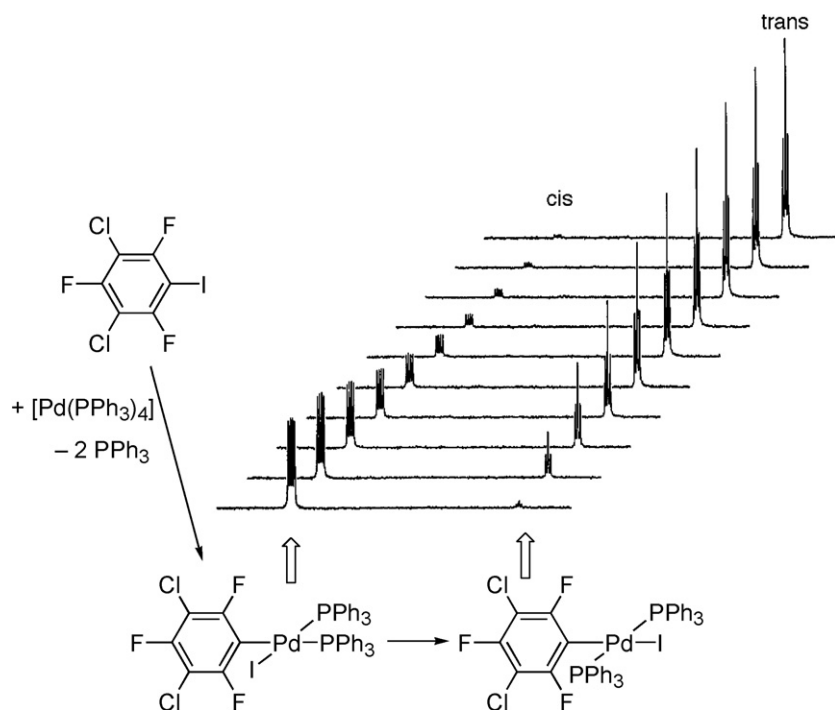


Fig. 27. Oxidative addition and isomerization of RfI to $[\text{Pd}(\text{PPh}_3)_4]$ as monitored by ^{19}F NMR at 10 min intervals. Only the region of F_{ortho} in the complexes is shown. Under the reaction conditions the oxidative addition is fast and has been already completed in the first recording. Reproduced with permission from ref. [71]. Copyright 1998, American Chemical Society.

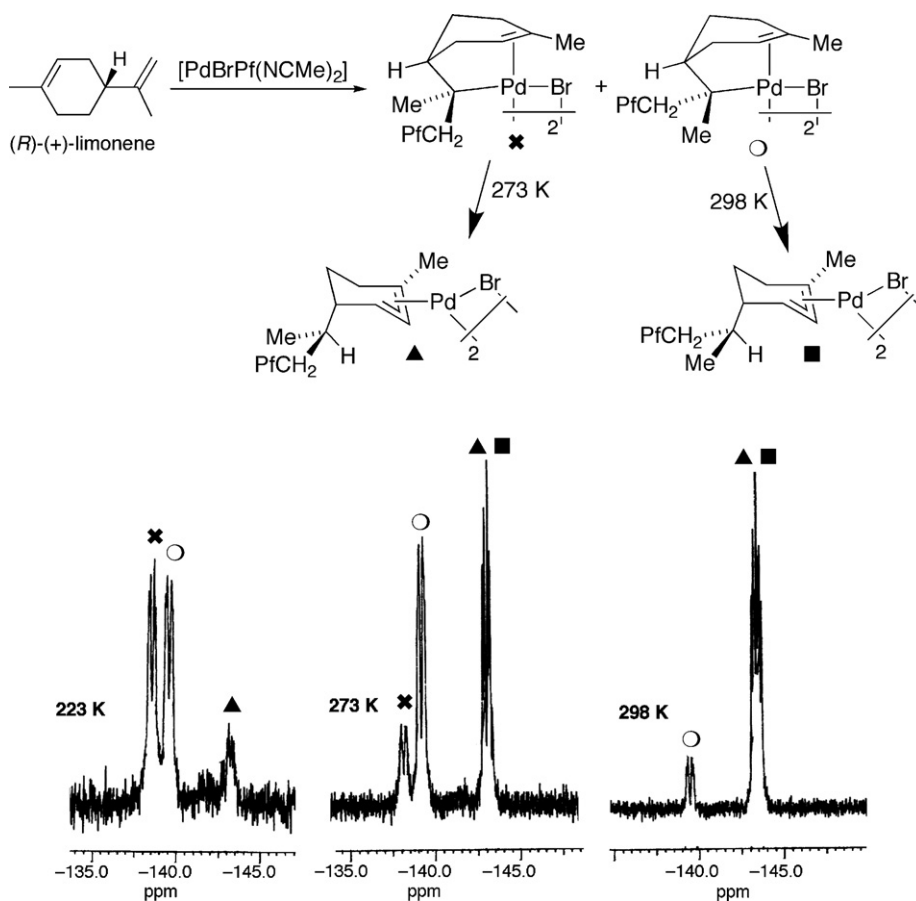


Fig. 28. ^{19}F NMR (F_{ortho} region) for the mixture of \times and \circ and snapshots of their conversion at different temperatures.

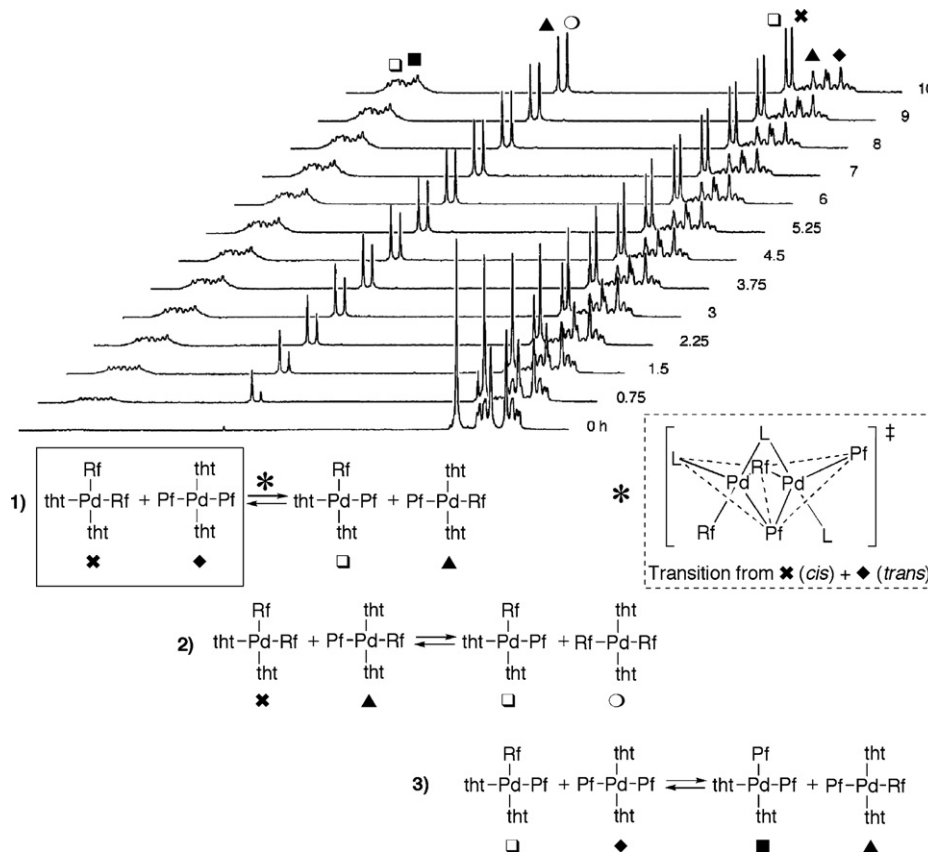


Fig. 29. ^{19}F NMR spectra of the reaction of $[\text{PdPf}_2\text{L}_2]$ with $[\text{PdRf}_2\text{L}_2]$ ($\text{L} = \text{tht}$) in the F_{ortho} region, at 45 min/1 h intervals. Compounds are labeled according to the scheme included. Reproduced with permission from ref. [12]. Copyright 1997, American Chemical Society.

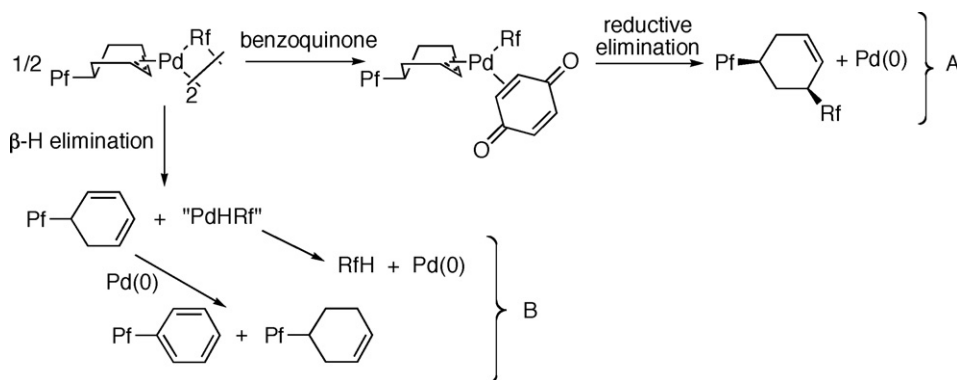
were not for the circumstance that both isomers transform into the allyls, as seen in Fig. 28, at very different rates, which could be determined [75].

4.4. Use of fluoroaryls to label several reaction partners

There are processes in solution that are blind to spectroscopic observation, unless some kinds of labeling are used. For instance, aryl exchange between palladium(II) centers (a process responsible for the formation of homocoupling byproducts in Pd-catalyzed C–C cross coupling reactions) cannot be seen when only one kind of molecule and R group is present, but their features become observable using two different R groups. Complexes $[\text{PdPf}_2\text{L}_2]$ and $[\text{PdRf}_2\text{L}_2]$ are almost thermodynamically identical and can be used to study aryl exchange, ligand exchange, and isomerization reactions. In fact all these processes are somehow related. The reaction of $[\text{PdPf}_2\text{L}_2]$ with $[\text{PdRf}_2\text{L}_2]$ (1:1) leads easily to the mixed $[\text{PdPfRfL}_2]$ in an almost statistical ratio when $\text{L} = \text{tht}$, SMe_2 , and it takes place with retention of the *cis* or *trans* configuration of the starting complexes [12]. This aryl exchange does not occur at comparable rates for other ligands such as $\text{L} = \text{PPh}_3$, AsPh_3 , picoline, COD. The process was studied by crossover experiments, using ^{19}F NMR that allows to detect distinctly complexes with different composition and stereochemistry, even in complicated mixtures. The results of one of these crossover experiments, mixing *cis*- $[\text{PdRf}_2\text{L}_2]$ with *trans*- $[\text{PdPf}_2\text{L}_2]$ are shown in Fig. 29, along with the sequence of

exchanges that explain the experimental results. The ^{19}F NMR kinetic study supports that the aryl groups scrambling takes place with retention of the configuration at both Pd centers in each step, via a triply-bridged binuclear activated complex $[\text{LRfPd}(\mu\text{-Rf})(\mu\text{-Pf})(\mu\text{-L})\text{PdPfL}]^\ddagger$ which was proposed based on a kinetic study using ^{19}F NMR. The third bridge in the activated complex uses a bridging S-donor ligand, which further supports the electron deficient aryl bridges, facilitating an otherwise difficult exchange (not observed for other L ligands, whether weak or strong, lacking a second lone pair). *cis*- $[\text{PdRfPfL}_2]$ and *trans*- $[\text{PdRfPfL}_2]$ are formed at the first stage of the reaction. As the reaction proceeds, exchange among the initial reactants and these initial products leads to the mixture of all possible isomers observed at the end of the reaction. Note that the formation of some of the products would suggest *cis*–*trans* isomerization, but they are in fact the result of aryl scrambling. *Cis*–*trans* isomerization of the starting complexes actually occurs, but at a much slower rate [93,94]. However it can be efficiently catalyzed by fluoroaryl gold(I) complexes, which get involved in fluoroaryl exchange with the Pd complexes [86].

The use of “flags” in the structure of compounds that can be easily identified has been a strategy used in ^1H NMR, i.e., with the introduction of methyl groups in specific parts of a molecule. ^{19}F NMR allows to do it in a more advantageous way: when information of the products arising from different reactants in a given process is needed, they can be labeled using different fluoroaryl groups in each molecule. The resonances in ^{19}F NMR



Scheme 12.

for each of them will appear distinctly and will give information of the fate of both reaction partners. The symmetrical Ar_F groups with simple spectral patterns Rf and Pf have been used for this purpose, as in the following examples.

The efficiency of the Stille coupling of allylic halides and aryltin derivatives is controlled by the reductive elimination, which is the slow step for this particular combination of reactants. The reaction was studied in detail and it was found that reductive elimination in the palladium η^3 -allyl complexes bearing an aryl group, formed as intermediates, must be promoted in order to get efficient coupling. A η^3 -allyl (μ -aryl) dimeric complex (Scheme 12), was independently prepared where aryl = Rf and the allyl moiety bears a Pf group. This complex decomposes upon heating by β -H elimination, and the products derived from the Rf and Pf-allyl groups are easily recognized (Scheme 12 and Fig. 30). Benzoquinone, an electron withdrawing ligand, was

then used as coupling co-catalyst and produced a clean reductive elimination, circumventing the coupling problems through the formation of a mononuclear complex with coordinated benzoquinone [72].

The precision of fluoroaryls to report on different but analogous species in solution is very well illustrated by the following example. The formation of two products observed by ^1H COSY in solutions of *trans*- $[\text{PdIPh}(\text{AsPh}_3)_2]$ in CDCl_3 , was assigned to an arsine dissociation equilibrium to give a tricoordinated species $[\text{PdIPh}(\text{AsPh}_3)]$ (22% at 293 K) [95]. The formation of such electron deficient molecule, or even a solvent-stabilized $[\text{PdIPh}(\text{AsPh}_3)(\text{CDCl}_3)]$ complex, is extremely unlikely compared to the alternative of forming a dimeric complex $[\text{Pd}_2(\mu\text{-I})_2\text{Ph}_2(\text{AsPh}_3)_2]$ upon arsine dissociation. In fact these dimeric complexes are easily prepared and crystallized. However, probing beyond discussion that they remain dimeric in solution is not easy. The strategy was to do a crossover experiment with $[\text{Pd}_2(\mu\text{-I})_2\text{Ph}_2(\text{AsPh}_3)_2]$ and $[\text{Pd}_2(\mu\text{-Cl})_2\text{Ph}_2(\text{AsPh}_3)_2]$. If they gave monomers (e.g. $[\text{PdIPh}(\text{AsPh}_3)(\text{CDCl}_3)]$) in solution, the NMR spectrum of the mixture should be the sum of the two components, but in case they remained dimers, new signals should appear corresponding to dimers with mixed bridges. The ^1H spectrum (Fig. 31) suggests in fact that some new signals appear, but the broad bands observed do not give much details.

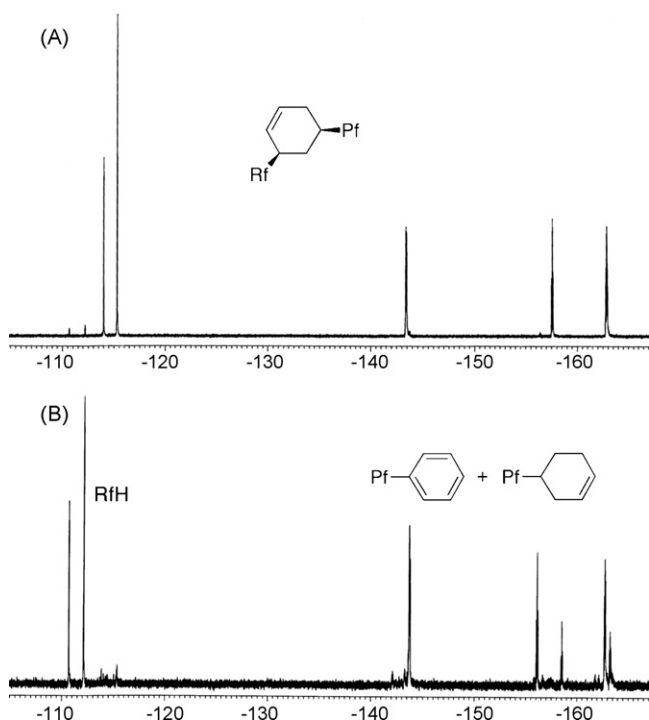


Fig. 30. (A) Coupling product obtained in the presence of benzoquinone, (B) Side products obtained in the absence of benzoquinone.

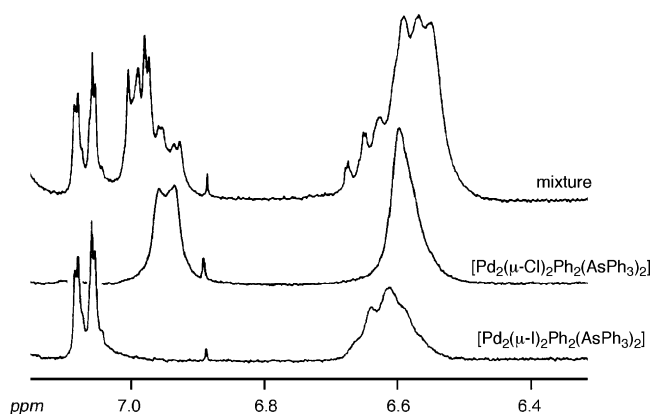


Fig. 31. ^1H spectra of CDCl_3 solutions of $[\text{Pd}_2(\mu\text{-I})_2\text{Ph}_2(\text{AsPh}_3)_2]$, $[\text{Pd}_2(\mu\text{-Cl})_2\text{Ph}_2(\text{AsPh}_3)_2]$ and an equimolecular mixture of both. Reproduced with permission from ref. [102]. Copyright 2002, Wiley.

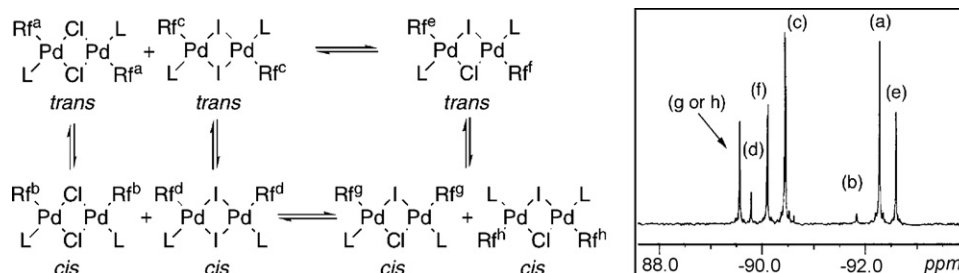
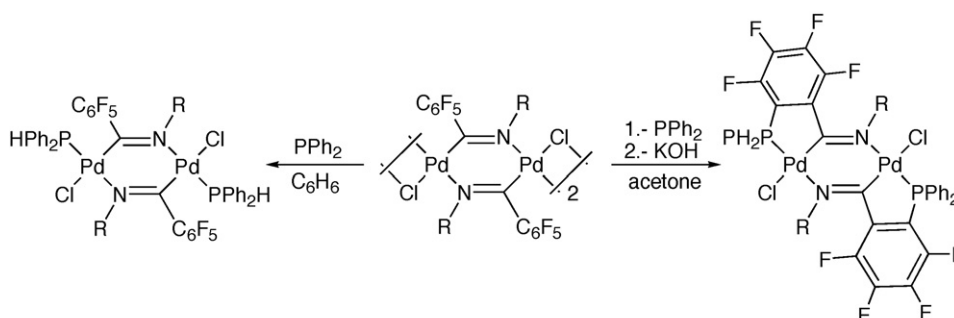


Fig. 32. ^{19}F NMR spectrum of an equimolecular mixture of $[\text{Pd}_2(\mu\text{-I})_2\text{Rf}_2(\text{AsPh}_3)_2]$, $[\text{Pd}_2(\mu\text{-Cl})_2\text{Rf}_2(\text{AsPh}_3)_2]$ in CDCl_3 . Only the range of the F_{ortho} signals is shown. The small symmetric signals flanking the high singlets are spinning sidebands. The signals are labeled as shown in the Scheme. Reproduced with permission from ref. [96]. Copyright 2002, Wiley.



Scheme 13.

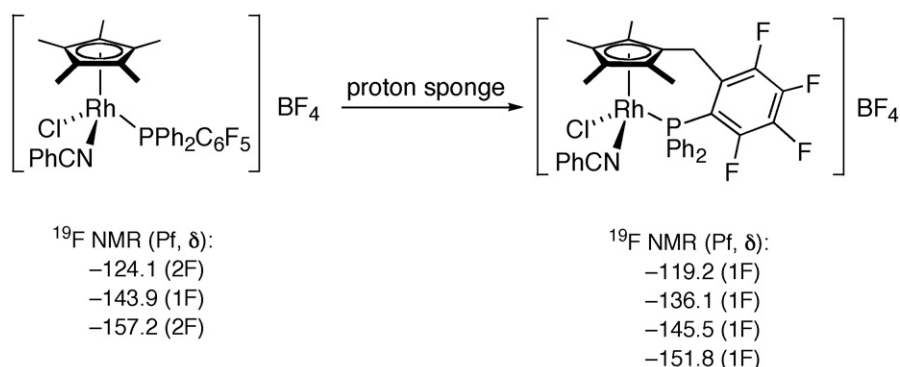
When the same study was carried out with the corresponding Rf complexes, the image was incredibly detailed. As shown in the scheme in Fig. 32, up to seven different dimers, giving rise to up to eight inequivalent Rf groups can be formed, arising from the different bridges and the *cis*–*trans* isomerism in the dimers. If the complexes were monomeric, only two signals should appear. The ^{19}F NMR spectrum in the F_{ortho} region shows seven lines distinctly, leaving no doubt of the dimeric nature of the complexes [96].

4.5. ^{19}F NMR in C–F activation processes

Many reactions of fluorocarbons or fluorocarbonyl groups with transition metals involving cleavage of C–F bonds have been described. Extensive accounts of this type of reactions have been published [97–99], and recent new examples can be found in the literature [100,101]. It is clear that the disappearance of a

fluorine atom in an organofluorine group, or its rearrangement in the molecule has a deep influence in the ^{19}F NMR spectrum and can be easily detected. Several examples are given below, most of them involving fluoroaryl groups or fluoroarenes although C–F activation processes for fluoroalkyls have also been reported [17,20,102,103].

The nucleophilic substitution of a fluorine atom in a fluoroaryl group is not uncommon [104–107]. Often the Ar_F group is part of a ligand not directly bonded to the metal and the metal plays a role in bringing the Ar_F group and the nucleophile close to each other, possibly reducing the activation entropy of the process. As a result, a new ligand is formed. For instance, the reaction of the tetranuclear imido bridged complex in Scheme 13 with PPh_2H in a non-polar solvent gives simply the usual reaction of Cl-bridge splitting. However, in a polar solvent and adding KOH to promote the formation of diphenylphosphide, the nucleophilic substitution of a F_{ortho} by PPh_2 is produced. The new complex



Scheme 14.

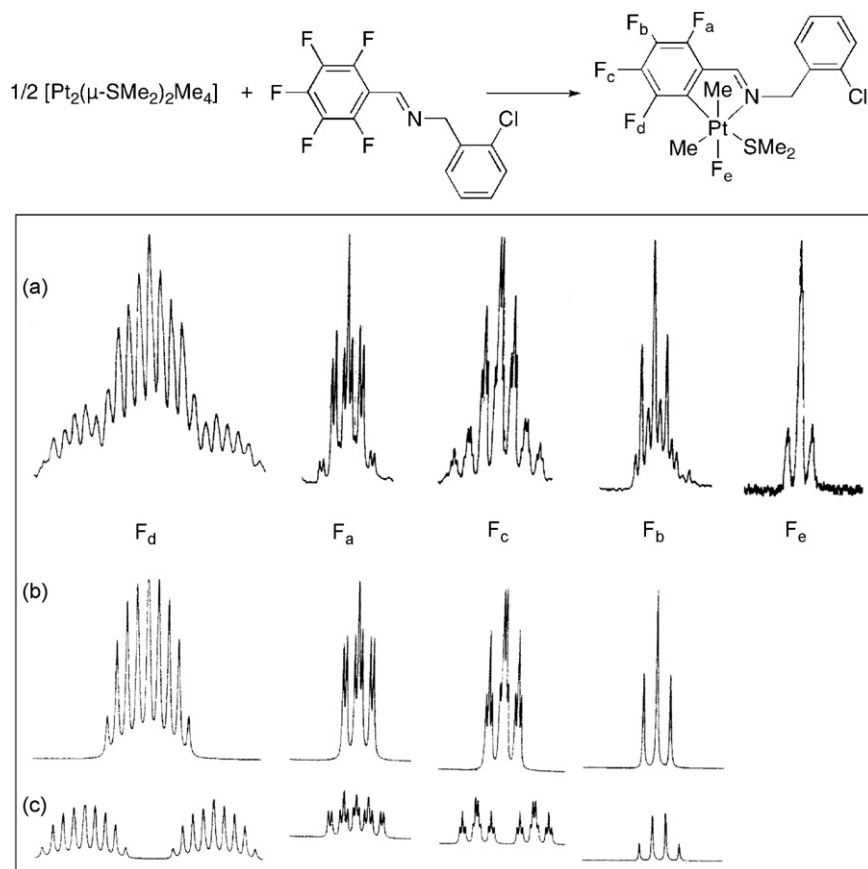


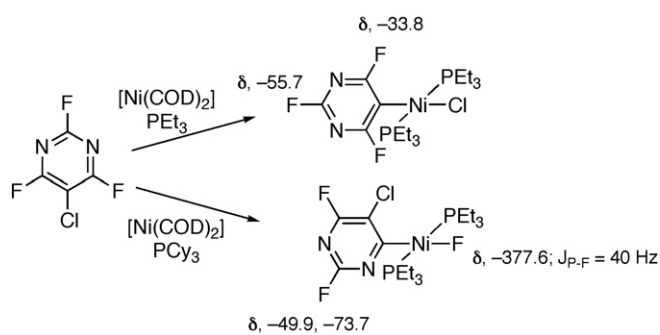
Fig. 33. ^{19}F NMR spectra of the orthometallated complex of Pt(IV) formed by C–F oxidative addition: (a) experimental, (b) simulated for the nonactive Pt isotopomer; (c) simulated for the ^{195}Pt isotopomer. Reproduced with permission from ref. [111]. Copyright 1993, American Chemical Society.

was easily identified by the observation of only four F resonances (1:1:1:1) and was confirmed by X-ray diffraction [104].

The new chelating ligand bound to rhodium in Scheme 14 is formed by fluorine nucleophilic substitution for the carbanion formed by deprotonation of one methyl of the Cp* ligand [106]. The three ^{19}F resonances associated with the pentafluorophenyl phosphine in the starting complex (free rotation of PF occurs) change to four resonances in a ratio (1:1:1:1) that clearly shows that a F atom has been lost.

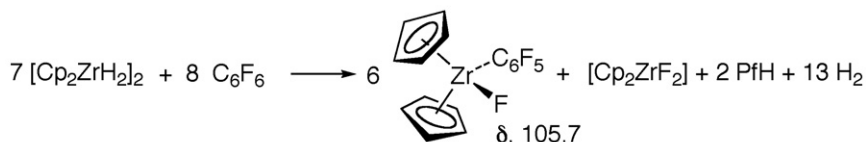
Oxidative addition reactions of C–F bonds of fluorinated aryls lead to new M–Ar_F and M–F bonds; the latter show distinct ^{19}F NMR chemical shifts that are decisive in order to identify the reaction. M–F resonances show a large range of chemical shift values [108]; for a given metal, these resonances are easily distinguished from other fluorine resonances in the molecule and hence they keep their structural significance.

The reaction of pentafluorophenyl Schiff bases with tungsten [109], or platinum [110,111] leads to fluorocomplexes



Scheme 15.

with tetrafluoroaryl substituted ligands, as a result of the oxidative addition. An example is shown in Fig. 33. The ^{19}F NMR spectrum of the Pt(IV) complex clearly reflects the presence of a Pt–F moiety (-259.4 ppm $^1J_{\text{Pt-F}} = 143$ Hz) and four resonances of the Ar_F moiety showing ^{195}Pt –F coupling. The



Scheme 16.

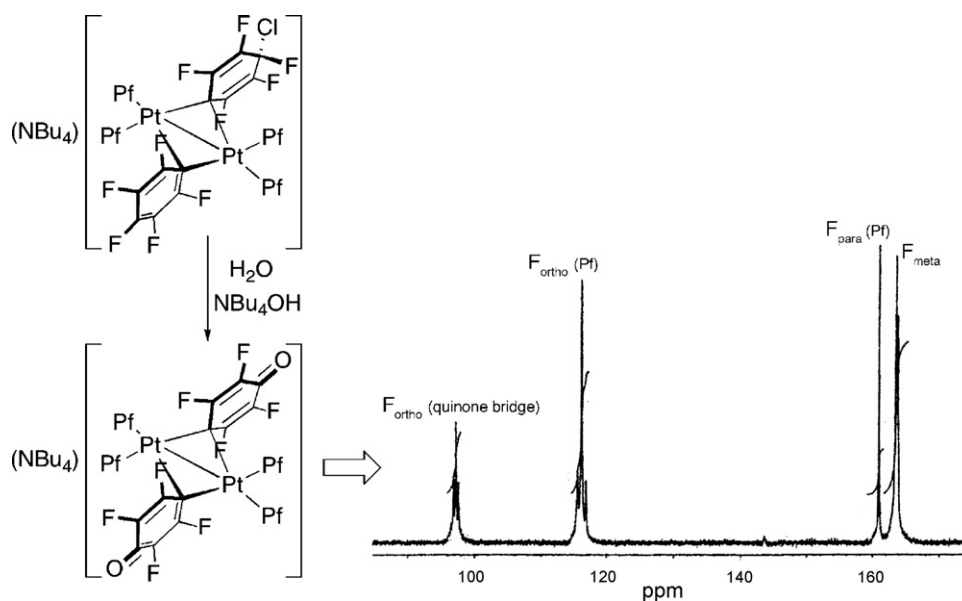
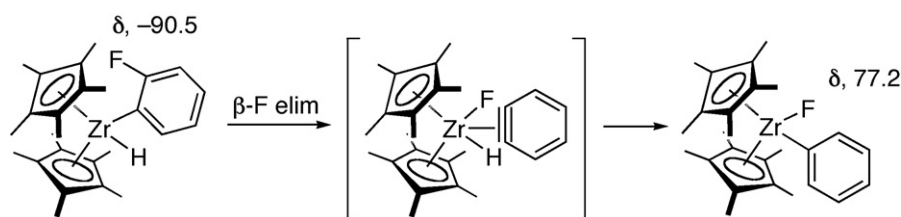


Fig. 34. C–X cleavage by nucleophilic attack in bridging fluoroaryls. The ^{19}F NMR spectrum of the final complex is shown. Reproduced with permission from ref. [25]. Copyright 1994, American Chemical Society.



Scheme 17.

experimental and simulated spectra are collected in the Fig. 33 [111].

As an example of reaction on a coordinated fluoroaryl, the nucleophilic attack of hydroxide on bridging fluoroaryl groups leads to an unusual Pt(III) complex with quinone-bridging ligands (Fig. 34) [25]. Two para C–F and a C–Cl bonds in the bridging aryls are cleaved and the ^{19}F NMR spectrum of the resulting complex shows the disappearance of the corresponding signals. Only one F_{para} resonance, corresponding to the terminal Pt groups, is observed. The F_{ortho} signals show typical chemical shifts for bridging (downfield shifted) or terminal arrangement.

Selective C–F or C–Cl oxidative addition has been observed in the reactions of halopyrimidines with $[\text{Ni}(\text{COD})_2]$ in the presence of phosphines depending on the PR_3 ligand used. Both situations are clearly distinguished using ^{19}F NMR (Scheme 15) [112].

Of great practical importance is the C–F activation of perfluorocarbons, such as hexafluorobenzene. Stoichiometric and catalytic reactions of this reagent with metal complexes have been reported [113]. The process shown in Scheme 16 is an example of activation of C_6F_6 [114]. It is noteworthy the large downfield shift observed for the Zr–F resonance, in contrast with the upfield shift typical of group 10 metal fluorides (see above).

C–F cleavage by a β -F elimination mechanism has also been reported for early transition metal centers [103]. The fate of the fluorine atom in the transformation shown in Scheme 17 can be

easily detected by ^{19}F NMR; it is proposed to occur via β -F elimination to give a benzyne complex, followed by benzyne insertion into the Zr–H bond [115].

5. Conclusions

The value of ^{19}F NMR spectroscopy is not limited to their natural objectives, the fluorinated compounds. Their characteristics make it a powerful technique to be applied to many chemical problems when the familiar ^1H and ^{13}C NMR spectroscopies find limitations, using fluorinated model compounds prepared for the purpose. This possibility should be taken into account when planning research, particularly in the fields of kinetics and reaction mechanisms.

Acknowledgements

This article is, in part, an account of personal work by the authors that could not have been carried out without the important contribution of all the co-workers who appear in the references. To them our greatest thanks, as well as to the projects supporting presently our present research: Project CTQ2007-67411/BQU and Project INTECAT Consolider Ingenio 2010 (CSD2006-0003), from the Ministerio de Educación y Ciencia.

Appendix A. Abbreviations

Ar	aryl
Ar _F	fluorinated aryl
BIP	2,6-bis[(1-phenylimino)ethyl]pyridine
Cp*	pentamethylcyclopentadienyl
COD	1,5-cyclooctadiene
Cy	cyclohexyl
dcy	dicyclopentadiene
dEpf	1,1'-bis(phenylthiol)ferrocene
dppf	1,1'-bis(diphenylphosphino)ferrocene
DIOP	2,3- <i>O</i> -isopropylidene-2,3-dihydroxy-1,4-bis(diphenylphosphino)butane
DMBI	3,3'-dimethyl-2,2'-biindazole
dmpz	3,5-dimethylpyrazolate
Fmes	2,4,6-tris(trifluoromethyl)phenyl
HH	head-to-head
HT	head-to-tail
indz	indazolate
LSA	line shape analysis
mpz	3-methylpyrazolate
MT	magnetization transfer
Me ₂ -TpzT	2,4,6-tris(3,5-dimethylpyrazol-1-yl)-1,3,5-triazine
NCN	[C ₆ H ₃ (CH ₂ NMe ₂)] [−]
Pf	pentafluorophenyl
Py	2-pyridyl
pz	pyrazolate
Rf	3,5-dichlorotrifluorophenyl
terpy	2,2':6,2''-terpyridine
tht	tetrahydrothiophene
Tol	tolyl
TPP	2,4,6-tris(2-pyridyl)pyrimidine
TPT	2,4,6-tris(2-pyridyl)-1,3,5-triazine

References

- [1] H. Günther, NMR Spectroscopy, Wiley, Chichester, 1987.
- [2] See, for instance E.F. Mooney, An Introduction to ¹⁹F NMR Spectroscopy, Heyden & Son Ltd., London, 1970.
- [3] M.A. Bennett, G.B. Robertson, A. Rokicki, W.A. Wickramasinghe, J. Am. Chem. Soc. 110 (1988) 7098 (and references therein).
- [4] P. Espinet, J.M. Martínez-Ilarduya, C. Pérez-Briso, A.L. Casado, M.A. Alonso, J. Organomet. Chem. 551 (1998) 9.
- [5] (a) A.J. Canty, in: E.W. Abel, F.G.A. Stone, G. Wilkinson (Eds.), Comprehensive Organometallic Chemistry, vol. 9, Pergamon Press, Oxford, 1995 (Chapter 5);
(b) P.M. Maitlis, P. Espinet, M.J.H. Russell, in: G. Wilkinson, F.G.A. Stone (Eds.), Comprehensive Organometallic Chemistry, vol. 6, Pergamon Press, Oxford, 1982 (Chapter 38.4);
(c) R. Usón, J. Forniés, Adv. Organomet. Chem. 28 (1988) 219.
- [6] C₆F₅Br can be purchased from many companies and 1,3,5-C₆Cl₃F₃ is available from Fluorochem on demand.
- [7] A.C. Albéniz, A.L. Casado, P. Espinet, Organometallics 16 (1997) 5416.
- [8] F. Gómez-de la Torre, A. de la Hoz, F.A. Jalón, B.R. Manzano, A.M. Rodríguez, J. Elguero, M. Martínez-Ripoll, Inorg. Chem. 39 (2000) 1152.
- [9] (a) F.B. Mallory, J. Am. Chem. Soc. 95 (1973) 7747;
(b) L. Ernst, K. Ibrom, K. Marat, R.H. Mitchell, G.J. Bodwell, G.W. Buschnell, Chem. Ber. 127 (1994) 1119.
- [10] L. Ernst, K. Ibrom, Angew. Chem. Int. Ed. Engl. 34 (1995) 1881.
- [11] M.A. Alonso, J.A. Casares, P. Espinet, J.M. Martínez-Ilarduya, C. Pérez-Briso, Eur. J. Inorg. Chem. (1998) 1745.
- [12] A.L. Casado, J.A. Casares, P. Espinet, Organometallics 16 (1997) 5730.
- [13] R. de la Cruz, P. Espinet, A.M. Gallego, J.M. Martín-Alvarez, J.M. Martínez-Ilarduya, J. Organomet. Chem. 663 (2002) 108.
- [14] P. Espinet, A.M. Gallego, J.M. Martínez-Ilarduya, E. Pastor, Inorg. Chem. 39 (2000) 975.
- [15] C. Bartolomé, P. Espinet, J.M. Martín-Alvarez, F. Villafañe, Eur. J. Inorg. Chem. (2004) 2326.
- [16] A.C. Albéniz, P. Espinet, C. Foces-Foces, F.H. Cano, Organometallics 9 (1990) 1079.
- [17] R.P. Hughes, R.B. Laritchev, L.N. Zakharov, A.R. Rheingold, J. Am. Chem. Soc. 127 (2005) 6325.
- [18] R.P. Hughes, D. Zhang, A.J. Ward, L.N. Zakharov, A.R. Rheingold, J. Am. Chem. Soc. 126 (2004) 6169.
- [19] R.P. Hughes, R.B. Laritchev, A. Williamson, C.D. Incavito, L.N. Zakharov, A.R. Rheingold, Organometallics 22 (2003) 2134.
- [20] S.A. Garratt, R.P. Hughes, I. Kovacic, A.J. Ward, S. Willemsen, D. Zhang, J. Am. Chem. Soc. 127 (2005) 15585.
- [21] A.C. Albéniz, P. Espinet, O. López-Cimas, B. Martín-Ruiz, Chem. Eur. J. 11 (2005) 242.
- [22] R. Usón, J. Forniés, M. Tomás, J.M. Casas, Organometallics 7 (1988) 2279.
- [23] R. Usón, J. Forniés, M. Tomás, J.M. Casas, R. Navarro, J. Chem. Soc. Dalton Trans. (1989) 169.
- [24] R. Usón, J. Forniés, M. Tomás, J.M. Casas, F.A. Cotton, L.R. Falvello, X. Feng, J. Am. Chem. Soc. 115 (1993) 4145.
- [25] R. Usón, J. Forniés, L.R. Falvello, M. Tomás, J.M. Casas, A. Martín, F.A. Cotton, J. Am. Chem. Soc. 116 (1994) 7160.
- [26] I. Ara, L.R. Falvello, S. Fernández, J. Forniés, E. Lalinde, A. Martín, M.T. Moreno, Organometallics 16 (1997) 5923.
- [27] L.R. Falvello, J. Forniés, C. Fortuño, F. Durán, A. Martín, Organometallics 21 (2002) 2226.
- [28] S.T. Belt, S.B. Duckett, M. Helliwell, R.N. Perutz, J. Chem. Soc. Chem. Commun. (1989) 928.
- [29] A.D. Selmeczy, W.D. Jones, M.G. Partridge, R.N. Perutz, Organometallics 13 (1994) 522.
- [30] R.J. Kulwiec, E.M. Holt, M. Lavin, R.H. Crabtree, Inorg. Chem. 26 (1987) 2559.
- [31] J. Karl, G. Erker, R. Frölich, J. Am. Chem. Soc. 119 (1997) 11165.
- [32] A.D. Horton, A.G. Orpen, Organometallics 10 (1991) 3910.
- [33] B.P. Patel, R.H. Crabtree, J. Am. Chem. Soc. 118 (1996) 13105.
- [34] J. Vicente, J. Gil-Rubio, D. Bautista, A. Sironi, N. Masciocchi, Inorg. Chem. 43 (2004) 5665.
- [35] J. Sandström, Dynamic NMR Spectroscopy, 2nd ed., Academic Press, London, 1982.
- [36] S. Coco, P. Espinet, J. Organomet. Chem. 484 (1994) 113.
- [37] (a) R. Baumgärtner, H.A. Brune, J. Organomet. Chem. 350 (1988) 115;
(b) T. Debaerdemaeker, C. Weisemann, H.A. Brune, J. Organomet. Chem. 350 (1988) 91.
- [38] G.K. Anderson, R.J. Cross, L. Malojlovic-Muir, K.W. Muir, M. Rocamora, Organometallics 7 (1988) 1520.
- [39] A.L. Rieger, G.B. Carpenter, P.H. Rieger, Organometallics 12 (1993) 842.
- [40] P.L. Alsters, J. Boersma, W.J.J. Smeets, A.L. Spek, G. van Koten, Organometallics 12 (1993) 1639.
- [41] J.M. Brown, J.J. Pérez-Torrente, N.W. Alcock, H.J. Clase, Organometallics 14 (1995) 207.
- [42] (a) J.M. Brown, J.J. Pérez-Torrente, N.W. Alcock, Organometallics 14 (1995) 1195;
(b) N.W. Alcock, J.M. Brown, J.J. Pérez-Torrente, Tetrahedron Lett. 3 (1992) 389.
- [43] G. Lu, H.C. Malinakova, J. Org. Chem. 69 (2004) 4701.
- [44] C.H.M. Amijs, A.W. Kleij, G.P.M. van Kink, A.L. Spek, G. van Koten, Organometallics 24 (2005) 2773.
- [45] R.L. Bennett, M.I. Bruce, R.C.F. Gardner, J. Chem. Soc. Dalton Trans. (1973) 2653.
- [46] G.B. Deacon, B.M. Gatehouse, K.T. Nelson-Reed, J. Organomet. Chem. 359 (1989) 267.

- [47] A.C. Albéniz, J.C. Cuevas, P. Espinet, J. de Mendoza, P. Prados, J. Organomet. Chem. 410 (1991) 257.
- [48] J. Ruiz, M.T. Martínez, C. Vicente, G. García, G. López, P.A. Chaloner, P.B. Hitchcock, Organometallics 12 (1993) 4321.
- [49] J. Forniés, R. Navarro, V. Sicilia, M. Tomás, Inorg. Chem. 32 (1993) 3675.
- [50] J. Forniés, F. Martínez, R. Navarro, E.P. Urriolabeitia, A.J. Welch, J. Chem. Soc. Dalton Trans. (1995) 2805.
- [51] (a) J. Forniés, F. Martínez, R. Navarro, E.P. Urriolabeitia, Organometallics 15 (1996) 1813;
(b) I. Ara, J.R. Berenguer, J. Forniés, E. Lalinde, M. Tomás, Organometallics 15 (1996) 1014;
(c) J. Forniés, M.A. Gómez-Saso, E. Lalinde, F. Martínez, M.T. Moreno, Organometallics 11 (1992) 2873;
(d) J.M. Casas, J. Forniés, A. Martín, B. Menjón, M. Tomás, J. Chem. Soc. Dalton Trans. (1995) 2949;
(e) J.R. Berenguer, J. Forniés, E. Lalinde, F. Martínez, E.P. Urriolabeitia, A.J. Welch, J. Chem. Soc. Dalton Trans. (1994) 1291;
(f) E.W. Abel, K.G. Orrell, A.G. Osborne, H.M. Pain, V. Sik, M.B. Hursthouse, K.M.A. Malik, J. Chem. Soc. Dalton Trans. (1994) 3341;
(g) J. Forniés, F. Martínez, R. Navarro, E.P. Urriolabeitia, A.J. Welch, J. Chem. Soc. Dalton Trans. (1993) 2147;
(h) U. Amador, E. Delgado, J. Forniés, E. Hernández, E. Lalinde, M.T. Moreno, Inorg. Chem. 34 (1995) 5279.
- [52] (a) L.R. Falvello, J. Forniés, R. Navarro, A. Rueda, E.P. Urriolabeitia, Organometallics 15 (1996) 309;
(b) J. Forniés, R. Navarro, E.P. Urriolabeitia, J. Organomet. Chem. 452 (1993) 241;
(c) J. Forniés, B. Menjón, N. Gómez, M. Tomás, Organometallics 11 (1992) 1187;
(d) G. López, J. Ruiz, C. Vicente, J.M. Martí, G. García, P.A. Chaloner, P.B. Hitchcock, R.M. Harrison, Organometallics 11 (1992) 4090;
(e) R. Usón, J. Forniés, M. Tomás, B. Menjón, A.J. Welch, Organometallics 7 (1988) 1318;
(f) J.M. Casas, L.R. Falvello, J. Forniés, A. Martín, Inorg. Chem. 35 (1996) 56;
(g) G. Sánchez, J. Ruiz, M.D. Santana, G. García, G. López, J.A. Hermoso, M. Martínez Ripoll, J. Chem. Soc. Dalton Trans. (1994) 19;
(h) G. López, J. Ruiz, G. García, C. Vicente, V. Rodríguez, G. Sánchez, J.A. Hermoso, M. Martínez Ripoll, J. Chem. Soc. Dalton Trans. (1992) 1681;
(i) G. López, G. Sánchez, G. García, J. García, A. Martínez, J.A. Hermoso, M. Martínez Ripoll, J. Organomet. Chem. 435 (1992) 193;
(j) J. Ruiz, F. Florenciano, V. Rodríguez, C. de Haro, G. López, J. Pérez, Eur. J. Inorg. Chem. (2002) 2736;
(k) J. Ruiz, V. Rodríguez, C. Vicente, J. Pérez, G. López, P.A. Chaloner, P.B. Hitchcock, Inorg. Chim. Acta 351 (2003) 114;
(l) J. Ruiz, V. Rodríguez, A. Pérez, G. López, D. Bautista, J. Organomet. Chem. 689 (2004) 2080;
(m) J. Ruiz, N. Cutillas, C. Vicente, M.D. Villa, G. López, J. Lorenzo, F.X. Avelés, V. Moreno, D. Bautista, Inorg. Chem. 44 (2005) 7365.
- [53] Free rotation of the fluoroaryl has been argued as the reason for equivalence even for molecules in which the square plane of the complex is a plane of symmetry, which makes both halves of the fluoroaryl ring equivalent by symmetry! See for instance references [52k,52l].
- [54] J.A. Casares, S. Coco, P. Espinet, Y.-S. Lin, Organometallics 14 (1995) 3058.
- [55] J.A. Casares, P. Espinet, J.M. Martínez-Ilarduya, Y.-S. Lin, Organometallics 16 (1997) 770.
- [56] J.A. Casares, P. Espinet, K. Soultantica, I. Pascual, A.G. Orpen, Inorg. Chem. 36 (1997) 5251.
- [57] A.C. Albéniz, A.L. Casado, P. Espinet, Inorg. Chem. 38 (1999) 2510.
- [58] P. Espinet, J.A. Casares, in: M. Gielen, R. Willem, B. Wrackmeyer (Eds.), Fluxional Organometallic and Coordination Compounds, Physical Organometallic Chemistry, vol. 4, Wiley, 2004 (Chapter 4).
- [59] J.A. Casares, P. Espinet, J.M. Martín-Álvarez, V. Santos, Inorg. Chem. 45 (2006) 6628.
- [60] J.A. Casares, P. Espinet, J.M. Martín-Álvarez, V. Santos, Inorg. Chem. 43 (2004) 189.
- [61] E.W. Abel, K.G. Orrell, A.G. Osborne, H.M. Pain, V. Sik, M.B. Hursthouse, K.M.A. Malik, J. Chem. Soc. Dalton Trans. (1994) 3441.
- [62] M.C. Carrión, A. Guerrero, F.A. Jalón, B.R. Manzano, A. de la Hoz, Inorg. Chem. 42 (2003) 885.
- [63] E.W. Abel, A. Gelling, K.G. Orrell, A.G. Osborne, V. Sik, Chem. Commun. (1996) 2329.
- [64] A. Gelling, M.D. Olsen, K.G. Orrell, A.G. Osborne, V. Sik, Chem. Commun. (1997) 587.
- [65] A. Gelling, M.D. Olsen, K.G. Orrell, A.G. Osborne, V. Sik, Inorg. Chim. Acta 264 (1997) 257.
- [66] E.W. Abel, K.G. Orrell, A.G. Osborne, V. Sik, M.W. da Silva, J. Organomet. Chem. 530 (1997) 235.
- [67] (a) S. Trofimenko, Chem. Rev. 93 (1993) 943;
(b) N. Kitajima, W.B. Tolman, Prog. Inorg. Chem. 43 (1995) 419;
(c) C. Slugovc, I. Padilla-Martínez, S. Sirol, E. Carmona, Coord. Chem. Rev. 213 (2001) 129.
- [68] (a) J.A. Casares, P. Espinet, Inorg. Chem. 36 (1997) 5428;
(b) J.A. Casares, P. Espinet, Inorg. Chem. 37 (1998) 2096.
- [69] A.C. Albéniz, P. Espinet, Y.-S. Lin, Organometallics 15 (1996) 5010.
- [70] J.A. Casares, P. Espinet, J.M. Martínez-Ilarduya, J.J. Mucientes, G. Salas, Inorg. Chem. 46 (2007) 1027.
- [71] A.L. Casado, P. Espinet, Organometallics 17 (1998) 954.
- [72] A.C. Albeniz, P. Espinet, B. Martín-Ruiz, Chem. Eur. J. 7 (2001) 2481.
- [73] A.C. Albeniz, P. Espinet, Y. Jeannin, M. Philoche-Levisalles, B. Mann, J. Am. Chem. Soc. 112 (1990) 6594.
- [74] A.C. Albeniz, P. Espinet, J. Organomet. Chem. 452 (1993) 229.
- [75] A.C. Albéniz, P. Espinet, Y.-S. Lin, Organometallics 14 (1995) 2977.
- [76] A.C. Albéniz, P. Espinet, R. Manrique, A. Pérez-Mateo, Chem. Eur. J. 11 (2005) 1565.
- [77] A.C. Albéniz, P. Espinet, A. Pérez-Mateo, A. Nova, G. Ujaque, Organometallics 25 (2006) 1293.
- [78] A.C. Albéniz, P. Espinet, Organometallics 10 (1991) 2987.
- [79] A.C. Albéniz, P. Espinet, Y.-S. Lin, J. Am. Chem. Soc. 118 (1996) 7145.
- [80] A.C. Albéniz, P. Espinet, Y.-S. Lin, Organometallics 16 (1997) 4138.
- [81] A.C. Albéniz, P. Espinet, Y.-S. Lin, Organometallics 16 (1997) 5964.
- [82] A.L. Casado, P. Espinet, J. Am. Chem. Soc. 120 (1998) 8978.
- [83] A.L. Casado, P. Espinet, A.M. Gallego, J. Am. Chem. Soc. 122 (2000) 11771.
- [84] A.L. Casado, P. Espinet, A.M. Gallego, J.M. Martínez-Ilarduya, Chem. Commun. (2001) 339.
- [85] J.A. Casares, P. Espinet, B. Fuentes, G. Salas, J. Am. Chem. Soc. 129 (2007) 3508.
- [86] A.L. Casado, P. Espinet, Organometallics 17 (1998) 3677.
- [87] A.C. Albéniz, P. Espinet, R. López-Fernández, Organometallics 25 (2006) 5449.
- [88] R. Usón, J. Forniés, P. Espinet, E. Lalinde, P.G. Jones, G.M. Sheldrick, J. Chem. Soc. Dalton Trans. (1982) 2389.
- [89] R. Usón, J. Forniés, P. Espinet, E. Lalinde, J. Organomet. Chem. 254 (1983) 371.
- [90] R. Usón, J. Forniés, P. Espinet, E. Lalinde, A. García, P.G. Jones, K. Meyer-Bäse, G.M. Sheldrick, J. Chem. Soc. Dalton Trans. (1986) 259.
- [91] R. Usón, J. Forniés, P. Espinet, E. Lalinde, P.G. Jones, G.M. Sheldrick, J. Organomet. Chem. 288 (1985) 249.
- [92] P. Espinet, A. Echavarren, Angew. Chem. Int. Ed. 43 (2004) 4704.
- [93] D. Minniti, Inorg. Chem. 33 (1994) 2631.
- [94] A.L. Casado, J.A. Casares, P. Espinet, Inorg. Chem. 37 (1998) 4154.
- [95] C. Amatore, A. Bucaille, A. Fuxa, A. Jutand, G. Meyer, A. Ndedi Ntepe, Chem. Eur. J. 7 (2001) 2134.
- [96] J. Casares, P. Espinet, G. Salas, Chem. Eur. J. 8 (2002) 4844.
- [97] J.L. Kiplinger, T.G. Richmond, C.E. Osterberg, Chem. Rev. 94 (1994) 373.
- [98] J. Burdeniuc, B. Jedlicka, R.H. Crabtree, Chem. Ber./Recueil. 130 (1997) 145.
- [99] W.D. Jones, Dalton Trans. (2003) 3991.

- [100] L. Maron, E.L. Werkema, L. Perrin, O. Eisenstein, R.A. Andersen, J. Am. Chem. Soc. 127 (2005) 279.
- [101] B.D. Bailey, J.C. Huffman, D.J. Mindiola, J. Am. Chem. Soc. 129 (2007) 5302.
- [102] J.D. Koola, D.M. Roddick, *Organometallics* 10 (1991) 591.
- [103] B.M. Kraft, W.D. Jones, J. Am. Chem. Soc. 124 (2002) 8681.
- [104] R. Usón, J. Forniés, P. Espinet, A. García, M. Tomás, J. Organomet. Chem. 282 (1985) C35.
- [105] S. Park, M. Pontier-Johnson, D.M. Roundhill, J. Am. Chem. Soc. 111 (1989) 3101.
- [106] R.M. Bellabarb, M. Nieuwenhuyzen, G.C. Saunders, *Organometallics* 21 (2002) 5726.
- [107] L. Villanueva, M. Arroyo, S. Bernès, H. Torrens, Chem. Commun. (2004) 1942.
- [108] N.M. Doherty, N.W. Hoffman, Chem. Rev. 91 (1991) 553.
- [109] T.G. Richmond, C.E. Osterberger, A.M. Arif, J. Am. Chem. Soc. 109 (1987) 8091.
- [110] C.M. Anderson, M. Crespo, G. Ferguson, A.L. Lough, R.J. Puddephatt, *Organometallics* 11 (1992) 1177.
- [111] M. Crespo, M. Martínez, J. Sales, *Organometallics* 12 (1993) 4297.
- [112] M.I. Sladek, T. Braun, B. Neumann, H.-G. Stammer, J. Chem. Soc. Dalton Trans. (2002) 297.
- [113] M. Aizenberg, D. Milstein, J. Am. Chem. Soc. 117 (1995) 8674.
- [114] B.L. Edelbach, A.K.F. Rahman, R.J. Lachicotte, W.D. Jones, *Organometallics* 18 (1999) 3170.
- [115] B.M. Kraft, R.J. Lachicotte, W.D. Jones, J. Am. Chem. Soc. 123 (2001) 10973.